Ana Cláudia Monteiro Marques

Licenciada em Biologia- Ramo de Biologia Molecular e Genética

The impact of Bridging Integrator 1 (BIN1) rare coding mutations on the development of Late-Onset Alzheimer's Disease

Dissertação para obtenção do Grau de Mestre em

Genética Molecular e Biomedicina

Orientador: Cláudia Guimas de Almeida Gomes

Investigadora Principal no Centro de Estudos de Doenças Crónicas (CEDOC)

Júri:

Presidente: Doutora Margarida Castro Caldas Braga

Arguente: Doutora Ana Sofia Falcão

Vogal: Doutora Cláudia Guimas de Almeida Gomes

FACULDADE DE CIÊNCIAS E TECNOLOGIA
UNIVERSIDADE NOVA DE LISBOA

Setembro de 2018

Universidade Nova de Lisboa

Faculdade de Ciências e Tecnologia

Departamento de Ciências da Vida

Ana Cláudia Monteiro Marques

Licenciada em Biologia- Ramo de Biologia Molecular e Genética

The impact of Bridging Integrator 1 (BIN1) rare coding mutations on the development of Late-Onset Alzheimer's Disease

Dissertação para obtenção do Grau de Mestre em

Genética Molecular e Biomedicina

Orientador: Cláudia Guimas de Almeida Gomes

Investigadora Principal no Centro de Estudos de Doenças Crónicas (CEDOC)

Setembro

2018

The impact of Bridging Integrator 1 (BIN1) rare coding mutations on the development of Late-Onset Alzheimer's Disease

Para a minha mãe

Acknowledgments

Para começar gostaria de agradecer à minha orientadora Cláudia Almeida por ter reconhecido o meu fascínio pelas neurociências e me ter aceite no grupo dela. No teu grupo senti que podia procurar a resposta para qualquer questão que me despertasse a curiosidade, dentro do racional é claro. Senti realmente que o único limite era aquele ao qual a nossa imaginação nos levava e que desde que sejamos empreendedores as barreiras são apenas meras oportunidades para nos ultrapassarmos. Obrigada por me teres integrado como um verdadeiro membro do laboratório e me teres mostrado sem reservas como tudo funciona. Agradeço ainda por me mostrares que com transparência e humildade todo o caminho é mais fácil.

Quero também agradecer às minhas colegas e mentoras Tatiana Burrinha, Farzané Mirfakhar, Catarina Perdigão e Inês Figueira.

Tatiana muito obrigada por toda a paciência que tiveste ao me ensinar todas as técnicas, mesmo nas alturas em que o trabalho era mais do que as horas do dia. Obrigada também por me apoiares sempre, pelos conselhos, e acima de tudo por me fazeres ver que o que eu muitas vezes achava que eram montanhas eram na realidade apenas lombas.

Catarina minha professora das "molecularices" muito obrigada por toda a ajuda e por coordenares o teu calendário preenchido com o meu de modo a eu poder aprender o máximo possível.

Inês, apesar de termos passado pouco tempo juntas a tua ajuda foi imprescindível. Obrigada por toda a alegria e cor que trouxeste contigo.

And last but not least, Farzané thank you very much for all your support and for teaching me not to stress about mistakes already made and things I cannot control. Thank you for all our talks and for sharing your knowledge and different perspectives on life, thanks to you I felt more understood and less alone.

To all four girls I know that karma will repay all your kindness and the patience you had with me, for which I am truly beyond grateful.

Um obrigada grande também às minhas colegas de trabalho. Apesar de não compreenderem bem este lado da minha vida sempre se esforçaram para o perceber e sempre me apoiaram com um inegável carinho. Conjugar o trabalho com a tese não foi nada fácil, mas convosco foi sem dúvida mais feliz. Por todos os "fechos" repletos de tolices e risos, 313 sempre.

Mónica Lopes, minha companheira do dia 1, obrigada por me inspirares a tentar ser uma versão melhor de mim. O teu sorriso permanente foi uma fonte de força constante.

Vanessa Correia obrigada por me ouvires, compreenderes e apoiares. Ouvir a tua perspectiva ajudou-me a manter a sanidade nas alturas mais difíceis.

Anaísa Sena a ti tenho de agradecer o desencaminhamento. Antes de começarmos a falar eu era uma pessoa que estava a rodar 6 pratos ao mesmo tempo. Graças a ti fui introduzida a uma nova cultura e os pratos caíram ao chão. Estou grata por isso, pois não sou sobre-humana e precisava de me re-focar de modo a terminar a maratona. Obrigada ainda por te revoltares comigo, e por tanta felicidade, foi mais do que essencial.

À minha família do Teatro Contra-Senso muito obrigada. Ter feito uma peça no meio de tudo o resto foi sem dúvida um desafio, mas como sempre um que me encheu o coração e a alma. O vosso apoio foi imprescindível e como sempre foi um prazer ter partilhado o palco convosco.

André Santos não podia deixar de te agradecer em particular. A tua fé inabalável em mim e nas minhas capacidades inspiraram-me a nunca desistir e a enfrentar cada desafio com a crença de que a vitória era mais do que possível. Obrigada por todo o carinho.

Ao André Amorim, obrigada por estares comigo desde o dia 1 de tantas aventuras. Ouvir as tuas histórias, tão excepcionalmente bem contadas, garantiram-me momentos de gargalhadas incontroláveis. Continuas a ser bem descrito pela palavra "especial".

À Joana Silva, minha companheira trans-Tejo, muito obrigada por estares lá durante todo o percurso. Obrigada por me compreenderes a 100% e eu só espero que tenhamos muitos mais momentos de partilha das peripécias, seguidas de risos. Que todas as pedras sirvam para construir um caminho melhor.

Ao João Silva obrigada por estares sempre lá sem qualquer hesitação e a qualquer momento. Provavelmente devo-te uns óculos por todos os longos textos que te fiz ler, mas tu sempre foste capaz de me ouvir e de me pôr um sorriso nos lábios. A vida contigo é mais fácil. Muito obrigada

À madrinha que a Faculdade de Ciências me deu, Sofia Silva, devo um enorme agradecimento. Obrigada por ouvires todos os meus desabafos e por me fazeres sempre sentir compreendida e apoiada. Estes desafios não foram fáceis, mas contigo ao meu lado foram certamente mais leves. Mil vidas não chegavam para te agradecer por tudo.

À minha família, obrigada não apenas pelo vosso amor e apoio durante esta fase, mas durante todos os momentos da minha existência. Se pudesse escolher não escolheria uma diferente, porque pessoas com corações maiores do que vocês, não encontraria. Amo-vos mais do que tudo.

Em último deixo o agradecimento mais importante. À minha mãe. Palavras nunca seriam suficientes para agradecer tudo o que fizeste por mim toda a minha vida. O mais importante neste momento é agradecer-te por nunca me deixares desistir e por apoiares todos os meus sonhos incondicionalmente. Sem ti mãe, eu não era nada.

Abstract

Late-onset Alzheimer's Disease (LOAD) is the most common cause of dementia. AD is characterized by the presence of neurofibrillary tangles and of amyloid plaques, mainly composed of β-amyloid peptides (Aβ). Aβ is generated intracellularly at early endosomes through the sequential cleavage of the amyloid precursor protein (APP) by two proteases, β-secretase (BACE1) and γ-secretase. This process is dependent on both APP and BACE1 endocytic trafficking. The Aβ peptide especially its longer form (Aβ42), is synaptotoxic.

Bridging integrator 1 (BIN1), an endocytic trafficking regulator, was identified through large genome-wide association studies to be the second-most prevalent genetic risk factor for LOAD, with the P318L and K358R mutations in *BIN1* having been found in increased frequency amongst AD patients. Moreover, BIN1 knockdown was found to increase Aβ42 generation by accumulating BACE1 at early endosomes. However, how two *BIN1* coding mutations lead to AD remains unknown. We hypothesized that these BIN1 mutations alter Aβ homeostasis, thus contributing to the development of LOAD.

Expression of BIN1 P318L, but not of BIN1 K358R, led to an increase in total BIN1, suggesting that the first mutation increases *BIN1* gene expression. Moreover, over-expression of mutant BIN1 not only increased Aβ42 accumulation but also altered the site of Aβ42 accumulation. We started investigating the mechanisms involved and found early endosomes with reduced levels of EEA1, a marker of early endosomes, in cells overexpressing BIN1 mutants. Finally, we found increased levels of BACE1 in cells overexpressing P318L, but decreased in cells overexpressing K358R, which suggests that they contribute to the development of AD through different pathways.

In conclusion, our research demonstrates that these SNPs do alter BIN1's normal functioning and lead to Aβ dyshomeostasis, the predominant model of AD pathogenesis. Nonetheless, the specific pathways whereby these mutations impact the production and/or clearance of Aβ42 still require further investigating.

Keywords: Alzheimer's disease, Bridging Integrator 1 (BIN1), Amyloid β (Aβ), amyloid precursor protein (APP), BACE1, intracellular trafficking.

Resumo

A doença de Alzheimer esporádica (DAE) é a causa mais comum de demência, sendo caracterizada pela presença de tranças neurofibrilares e de placas senis, compostas principalmente por β-amilóide (Aβ). A Aβ é gerada intracelularmente nos endossomas iniciais pela clivagem da proteína percursora amilóide (APP) por duas protéases: β-secretase (BACE1) e γ-secretase. Este processo depende do tráfego intracelular destas proteínas. A Aβ, especialmente a sua maior forma (Aβ42), é sinaptotóxica.

O Bridging Integrator 1 (BIN1) é um regulador do tráfego endocítico, identificado por estudos de associação genómicos como o segundo principal fator de risco genético para DAE. O silenciamento do BIN1 aumenta a geração de Aβ42 devido à acumulação de BACE1 nos endossomas iniciais. As mutações P318L e K358R no BIN1 foram encontradas em elevada frequência entre pacientes com DAE, no entanto, o modo como estas mutações provocam esta doença é desconhecido. A nossa hipótese é que estas alteram a homeostase da Aβ, levando assim ao desenvolvimento da doença.

A expressão da P318L aumentou o BIN1 total, sugerindo que esta mutação aumenta a expressão do gene. A sobreexpressão dos mutantes aumentou a acumulação de Aβ42 e alterou a localização desta acumulação. Uma investigação inicial dos mecanismos envolvidos demonstrou níveis reduzidos de EEA1 nos endossomas iniciais das células a sobreexpressar os mutantes. Por fim, vimos um aumento dos níveis da BACE1 nas células a sobreexpressar P318L, mas um nível diminuído nas que sobreexpressavam K358R, o que pode significar que estas mutações contribuem para o desenvolvimento de DA através de vias diferentes.

Concluindo, a nossa pesquisa demonstra que estas mutações alteram o funcionamento normal do BIN1, levando à dishomeostase da Aβ. Esta dishomeostase é o modelo predominante da patogénese da DA. Ainda assim, as vias especificas através das quais a produção e/ou eliminação da Aβ42 está a ser afetada necessita de investigação adicional.

Palavras-chave: Doença de Alzheimer, Bridging Integrator 1 (BIN1), β-amilóide (Aβ), proteína precursora amilóide (PPA), BACE1, tráfego intracelular.

Index

Index of Figures

Index of Tables

Abbreviations

AD	Alzheimer's Disease
AICD	APP intracellular domain
ANOVA	Analysis of Variance
AP-2	Adaptor Protein-2
APP	Amyloid precursor protein
APPsα	Soluble APP cleaved by α-secretase
APPsβ	Soluble APP cleaved by β-secretase
Aβ	Amyloid β
Aβ40	Amyloid β (40 amino acids)
Aβ42	Amyloid β (42 amino acids)
BACE1	β-site APP-cleaving enzyme 1
BAR	BIN-Amphiphysin-Rvs
BIN1	Bridging Integrator 1
cDNA	complementary DNA
CLAP	Clathrin-Adaptor Protein
CO_2	Carbon dioxide
CTF	Carboxyl-terminal fragment
EEA1	Early endosomal antigen 1
ELISA	Enzyme-Linked Immunosorbent Assay
EOAD	Early-onset AD
FBS	Fetal bovine serum
GFP	Green Fluorescence Protein
GTP	Guanosine triphosphate
GWAS	Genome Wide Association Studies
HRP	Horseradish peroxidase
IF	Immunofluorescence
LAMP1	Lysosomal-associated membrane protein 1
LB	Luria Bertani (medium)
LOAD	Late-onset AD
mRNA	Messenger ribonucleic acid
N2a	Neuro 2a
PBS	Phosphate buffered saline
RIPA	Radio-Immunoprecipitation Assay

RNAi	RNA-mediated interference
SDS	Sodium dodecyl sulfate
SEM	Standard Error of the Mean
SH3	Src homology 3
siRNA	Small interference RNA
SNP	Single nucleotide polymorphism
WB	Western Blot
α-CTF	α-carboxyl-terminal fragment
β-CTF	β-carboxyl-terminal fragment

I. Introduction

1. The discovery of AD

In November 1901 Alois Alzheimer described the symptoms he had observed in a patient committed at the time to the Frankfurt Psychiatric Hospital, Auguste Deter (Hippius, 1998). This 51 year-old-woman displayed paranoid characteristics, with auditory hallucinations and aggressiveness, as well as disorientation not only in space but also in time. Soon after her internment to the hospital she started developing rapid memory loss until this symptom was so severe that it impeded her speaking ability and her recollection of how to use certain objects. Despite all these symptoms most of her motor skills, like her walk and the use of her hands, remained unaffected (Stelzma *et al.*, 1995; Hippius, 1998).

This patient passed away four and a half years after her arrival at the psychiatric hospital. At the time of her passing she was completely bedridden. At this point Alzheimer was able to perform an autopsy with the objective of trying to find the cause for the symptomatology exhibited. He examined the brain both morphologically as well as histologically (Stelzma *et al.*, 1995).

Macroscopically the first thing he observed was that the brain was evenly atrophied, meaning that there were no specific focal areas of degeneration. Alzheimer's histological observation was made utilizing Bielschosky's silver method which had been improved from the previous method developed by Ramon Y Cajal (Uchihara, 2007). Through this method he saw that approximately 1/3 of all the cortex neurons presented specific changes in the form of one or more fibrils. These neurofibrils were easily identified due to their thickness and capacity for impregnating the dye (Stelzma *et al.*, 1995). Alzheimer's descriptions of his observations correspond to what is now known as neurofibrillary tangles and amyloid plaques.

Even though the connection that this doctor made between the clinical symptoms and the histological observations were something never before seen, there was a huge lack of response as it was still a very rare disease (Hippius, 1998). In the end of his publication, Alzheimer noted that there was an increasing number of similar cases emerging and that this fact should encourage psychiatrists to try and discover new psychiatric illnesses instead of only noting the ones already in textbooks. Additionally, he also mentions the importance of histological examinations, as a way to further characterize these diseases (Stelzma *et al.*, 1995).

In 1911 Alzheimer published about another patient, Josef F., diagnosed as having the condition already named Alzheimer's disease (AD). This patient further expanded the knowledge of this condition because the histological examination showed only the presence of plaques but not of neurofibrillary tangles. This finding was very contradictory at the time since two different observations were being

classed as belonging to the same disease (Hippius, 1998). In 1995 the brain slide preparations of Auguste D. and Josef F. were re-examined with more modern techniques and it was concluded that cases presenting only plaques and cases with both plaques and tangles corresponded to different stages in the disease progression (Graeber *et al.*, 1997). This means that not only did Alois Alzheimer first discover the disease, but that he also noted that there were different development stages with the deposition of plaques occurring in an earlier stage than the emergence of neurofibrillary tangles.

2. AD pathology

Affecting over 40 million patients worldwide, AD which was virtually unknown to the general population, is now recognized as the most common dementia in the elderly (Selkoe and Hardy, 2016). Dementia is the clinical term used when referring to progressive cognitive decline which leads to an inability to perform normal day-to-day activities (O'Brien and Wong, 2011).

The true number of people affected by this condition isn't known, not only due to the fact that the disease actually begins in the brain nearly three decades before diagnosis is even possible (Selkoe and Hardy, 2016), but also due to the challenge of diagnosis itself since differentiating between AD and cognitive decline related with normal aging may be difficult. In fact dementia affects 1 out of 3 elderly individuals (O'Brien and Wong, 2011). Nonetheless, it is estimated that by 2050 the number of AD patients worldwide may reach approximately 144 million (Gomez-Ramirez and Wu, 2014).

Like Alois Alzheimer had firstly identified, this complex multifactorial syndrome is characterized by the presence of two distinct brain pathologies: neuritic plaques, composed mostly of amyloid β (Aβ) peptides, which are a chain of most commonly 40-42 amino acids (Masters *et al.*, 1985), surrounded by dystrophic neuronal processes (O'Brien and Wong, 2011) and neurofibrillary tangles which consist of intracellular, hyperphosphorylated and cleaved forms of tau (Iqbal and Grundke-Iqbal, 2008) (**Figure I.1**). Tau is a heat stable protein essential for microtubule assembly and stabilization (Weingarten *et al.*, 1975). When tau protein is misfolded due to these abnormal modifications, it dissociates from microtubules and aggregates in bundles of filaments (Iqbal *et al.*, 2010).

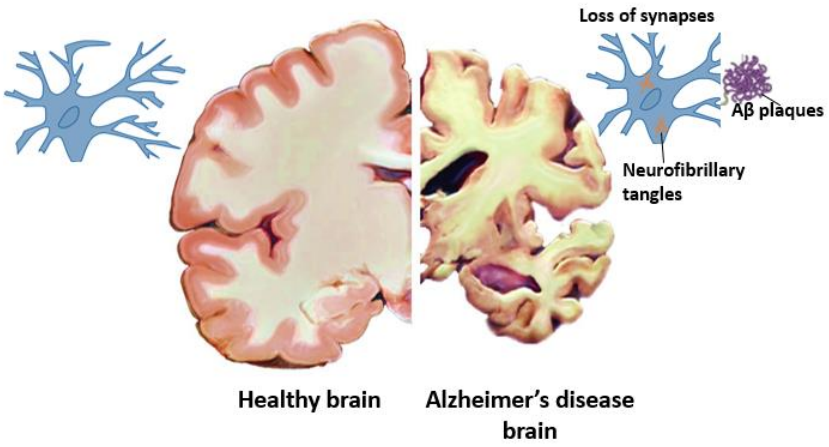

Figure I.1- Neuropathological features of the AD brain. Comparison between the normal brain (left side) and neurons to the pathological alterations that occur due to AD (right side: neurofibrillary tangles, neuritic plaques and general brain atrophy). Image adapted from Congdon and Sigurdsson, 2018.

The progressive buildup of protein aggregates in various systemic organs has been named as the cause for numerous other neurodegenerative diseases like Parkinson's disease and Creutzfeldt–Jakob disease (Lee *et al.*, 2011). The predominant model of AD pathogenesis is the amyloid (or Aβ) hypothesis in which it is proposed that this illness is initiated by Aβ dyshomeostasis (Hardy *et al.*, 1992), whether due to an excess in its production or a defect in its clearance. One aspect that supports this hypothesis is the observation that Aβ generation and deposition in humans precedes the accumulation of neurofibrillary tangles (Bateman *et al.*, 2012), whereas mutations in the tau gene were not seen to lead to Aβ accumulation (Lewis *et al.*, 2001). This implies that while the increase of Aβ possibly leads to progressive tau deposition, the opposite does not occur, thus further supporting the amyloid hypothesis.

3. APP processing

Amyloid precursor protein (APP) is a ubiquitous membrane protein synthesized in the endoplasmic reticulum (ER). Similarly to other membrane proteins, a fraction of the APP produced is transported to the cell surface via the secretory pathway, while some is directed to an endosomal compartment (O'Brien and Wong, 2011; Rajendran and Annaert, 2012).

APP's physiological function is not fully known, however, when transiently transfecting cell lines with APP, it was seen that this protein is able to modulate cell motility and growth, as well as neurite growth and cell survival (Thinakaran and Koo, 2008).

This ubiquitous protein is abundantly produced in neurons and as such it is metabolized rapidly through several proteolysis pathways (O'Brien and Wong, 2011). One of these metabolization pathways is the sequential cleavage by two amyloidogenic proteases: β-secretase and γ-secretase. This process leads to the generation of Aβ and is known as the amyloidogenic pathway. Cleavage by these secretases occurs not only in people with AD but also, in reduced amounts, in the physiological state. However, the main processing pathway of APP involves a different protease: α-secretase. Cleavage by α-secretase

followed by processing by γ-secretase does not lead to the formation of Aβ peptides and is thus known as the non-amyloidogenic pathway. This occurs because the cleaving location of α-secretase is within the normal sequence of Aβ, therefore not allowing its production (O'Brien and Wong, 2011) (**Figure I.2**). Aβ peptide size varies from 38 to 43 amino acids, depending on γ-secretase cleavage site, with the 40 and 42 amino acids types being the most common and reported (Rajendran and Annaert, 2012).

One of the factors that dictates which pathway is taken has to do with the location of APP. Proteolysis by α-secretase occurs mainly on the cell surface, while the neuronal β-secretase (BACE1) is primarily localized to endosomal compartments and therefore this is where the formation of most of the Aβ protein happens (O'Brien and Wong, 2011). This means that any factor that disrupts the normal trafficking of APP, increasing the time it spends in either of these cellular locations, or the amount of protein being sent there, benefits either the amyloidogenic of the non-amyloidogenic pathway.

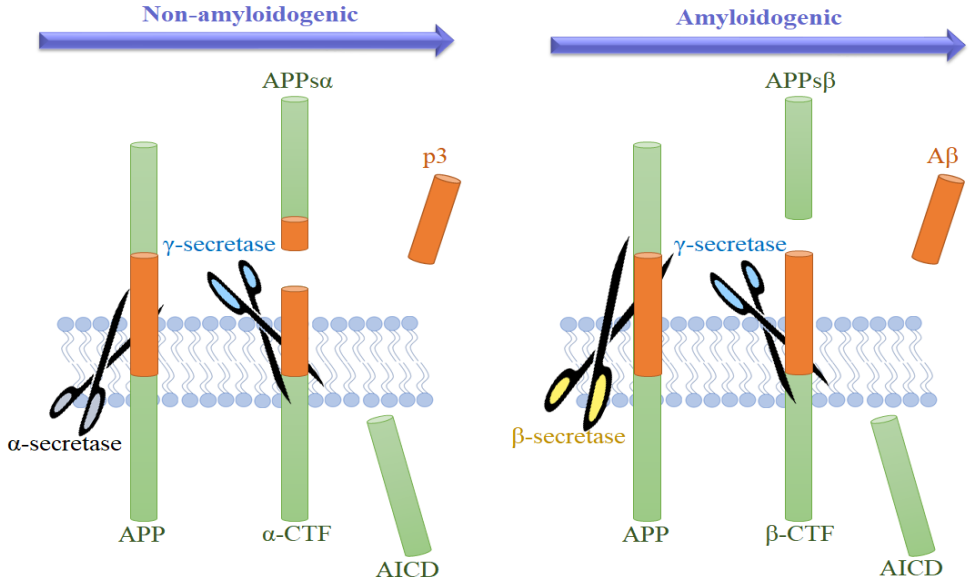

Figure I.2- APP processing through the non-amyloidogenic and the amyloidogenic pathways. Metabolization of the APP protein in the physiological state mainly involves its cleavage by α-secretase in the cellular membrane leading to the formation of α-CTFs, which will be further cleaved by γ-secretase in early endosomes resulting in the production of the AICD fragment. This is known as the non-amyloidogenic pathway, however, in smaller portions, APP can be firstly cleaved by β-secretase (BACE1) in the cell membrane, resulting in β-CTFs, and then by γ-secretase. This last cleavage step is the one which results in the production of Aβ.

4. Endosomes

Endosomes are cellular organelles responsible for the sorting of membrane-associated proteins (Weering and Cullen, 2014). Even though both BACE1 and APP are transported from the cell membrane to early endosomes, they use different routes, with APP being internalized in a clathrin-dependent way while BACE1's internalization involves GTPases (Chia *et al.*, 2013). This segregation between APP and BACE1 is partly responsible for limiting the amount of Aβ that is normally produced. Another

factor that might limit BACE1 cleaving activity to endosomes is that its proteolytic activity is optimal at a slightly acidic pH, making the endosomal environment optimal for this process (Morel *et al.*, 2014).

Early endosomes, as the name suggests, are the first endocytic compartment to accept cargo derived from the plasma membrane, beginning process known as early-to-late endosome maturation (Scott *et al.*, 2014). This is the process that ultimately results in the sorting of different proteins and lipids, through several different trafficking routes (Weering and Cullen, 2014). In some cases, like with APP, the endosomal maturation process proceeds until components are ultimately sent for degradation in the lysosome, while in others there can be a retrieval of cargoes, which are then sent to the biosynthetic pathway in the *trans*-Golgi network, or recycled back to the cellular membrane, as is the instance for BACE1 (Morel *et al.*, 2014; Weering and Cullen, 2014).

5. Amyloid hypothesis

The hypothesis that the pathological processes that ultimately lead to AD starts by a dishomeostasis of the Aβ protein is known as the amyloid hypothesis. This theory is supported by the fact that mutations in presenilin 1 or 2, the catalytic subunits of γ-secretase, are the most common cause of early-onset AD (EOAD), also known as familiar AD, which affects people under the age of 65 (Selkoe and Hardy, 2016). This type of AD is also commonly correlated with mutations in the APP gene, most of which are located near the γ-secretase cleavage site (O'Brien and Wong, 2011; Selkoe and Hardy, 2016), however, the most well-known APP mutation is next to the BACE1 cleavage site (APP-swe) (O'Brien and Wong, 2011). Both presenilin and APP mutations lead to an increase in total Aβ or to an increase in the Aβ42/Aβ40 ratio. Increasing the ratio between Aβ42 and Aβ40 boosts plaque formation since the Aβ42 peptide is more synaptotoxic due to it being more hydrophobic and prone to aggregation, which ultimately results in more Aβ deposition (Peric and Annaert, 2015; Selkoe and Hardy, 2016).

One important factor to mention is the toxicity of the Aβ peptide. This toxicity was well demonstrated in neuronal cultures derived from the hippocampus to which medium containing Aβ was added. This increase in extracellular Aβ led to neuronal degeneration after 24 hours, with complete neuronal loss within 48 to 72 hours (Yankner *et al.*, 1989). Regarding *in vivo* experiments, 4 to 6 month mice overexpressing mutant human APP showed a deposition of Aβ, and consequently presented with neuronal injuries (Shankar *et al.*, 2008).

In the beginning of the study of AD, and still to this day, some investigators raise questions as to which is the most important and impactful protein: Aβ or tau? What is however important to note is that Aβ has been shown to control both cleavage (Chung *et al.*, 2001) and phosphorylation (Hernández and Avila, 2008) of tau through its ability to activate some of the caspases and kinases involved in this process. As previously mentioned this is important because it is this form of the tau protein that

composes the neurofibrillary tangles. Reduction of Aβ levels through immunotherapy was shown to prevent tau pathology (Billings *et al.*, 2005).

6. Genetics of AD

The most frequent type of AD is known as late-onset AD (LOAD), due to the fact that its onset occurs after 65 years of age. Unlike EOAD, LOAD is sporadic and not caused solely by genetic mutations that result in fully penetrant AD. Nonetheless, it is estimated that LOAD is 50% to 70% caused by some genetic factor or by a combination of genetic components (O'Brien and Wong, 2011).

LOAD is usually correlated with either an imbalance in the Aβ42/Aβ40 ratio or with a decrease in Aβ clearance. There are a few identified causal factors related with this disease including the best-known apolipoprotein E4 (*ApoE4*) allele, which was first discovered in 1993 (Corder *et al.*, 1993). The *APOE* gene has three different variants which encode for the ApoE2, ApoE3 and ApoE4 proteins. ApoE protein has several physiological roles, including its ability to bind Aβ (Tiraboschi *et al.*, 2004). Unlike the other two forms of the protein, ApoE4 is not able to tightly bind Aβ (Tokuda *et al.*, 2000) and this is one of the reasons why heterozygous carriers of this allele (people who only carry one copy of it) have a threefold increase in their risk of developing AD. Homozygous carriers of this gene are 15 times more likely of developing this illness (O'Brien and Wong, 2011). Individuals who carry this allele have a decrease in the clearance of Aβ, which in turn promotes its aggregation leading to an increased risk for AD (Selkoe and Hardy, 2016). Other *loci* reported to increase the risk for LOAD are much weaker in effect (Lambert et al, 2013) or much rarer (Guerreiro et al, 2013; Jonsson et al, 2013).

Large genome-wide association studies (GWAS) (Feero *et al.*, 2010) have identified nine other genes/*loci* associated with an increase in the genetic risk for LOAD (Tan *et al.*, 2013). Some of these are involved in the regulation of endosomal recycling, as is the case for sortilin-related receptor 1 (SorL1), CD2-associated protein (CD2AP), phosphatidylinositol binding clathrin assembly protein (PICALM) and bridging integrator 1 (BIN1) (Cormont *et al.*, 2003; Andersen *et al.*, 2006; Pant *et al.*, 2009; Kanatsu *et al.*, 2014)**.** SORL1 has been shown to be involved in the processing of APP (Andersen *et al.*, 2006)**,** preventing the interaction between this protein and BACE1 by promoting the transport of APP from endosomes, where this interaction occurs, to the Golgi (O'Brien and Wong, 2011). This means that a reduction of SorL1 potentiates Aβ production. PICALM seems to be involved directly in endosomal APP processing (Kanatsu *et al.*, 2014) and has been implicated in the transport of brain Aβ across the blood-brain barrier (Zhao *et al.*, 2016). This means that a decrease in PICALM levels should lead to a defect in Aβ clearance, thereby leading to a higher change of developing AD. However, it was also seen that due to PICALM's role in the endocytosis of γ-secretase, its loss leads to a shift in the location of this protease, which then results in a decrease in production of Aβ42 (Kanatsu *et al.*, 2014).

Bridging integrator 1 (BIN1) and CD2AP are two other proteins that present as possible risk factors for AD development, however their involvement in the pathways leading to AD isn't as well-known as some of the other risk factors (Tan *et al.*, 2013).

7. Bridging integrator 1 (BIN1)

BIN1 also known as amphiphysin 2 is encoded on chromosome 2q14.3 and its transcripts suffer differential splicing according to tissue distribution. There are ten different BIN1 isoforms, being that seven of them are brain specific, one expressed in the skeletal muscles and the final two are ubiquitous forms. The fact that there are numerous variants of this protein is suggestive of a likelihood of several different physiological functions (Tan *et al.*, 2013)**.** BIN1 was initially characterized for its function as a tumor suppressor, seeing as it is a crucial member of the pathways leading to a caspase-independent cell death similar to apoptosis (Elliott *et al.*, 2000).

Despite the existence of different forms of this protein, most of them have in common an N-terminal BAR domain, a Myc-interacting domain and a C-Terminal SH3 domain. The brain variants also include a very interesting domain, the clathrin-AP2 binding domain (CLAP) which mediates the interaction between clathrin and AP2/α-adaptin (Tan *et al.*, 2013). The BAR domain has the ability of binding lipid membranes and inducing membrane curvature, thus enabling this protein to intervene in cellular trafficking events. This domain is part not only of BIN1 but also of other different proteins (Ren *et al.*, 2006). Besides its role in regulating the shape of membranes, the BAR domain also interacts directly with actin-binding proteins and with actin filaments themselves. Human BIN1, specifically, was seen to not only interact directly with actin filaments but to also be sufficient for F-actin binding, contributing to the stabilization of this protein, all of this mediated through the BAR domain of this protein (Dräger *et al.*, 2017). Interaction with actin could grant BIN1 not only an involvement in cell morphogenesis, but also another pathway for its involvement in controlling trafficking events.

Evidence regarding BIN1's involvement in AD includes a correlation between higher levels of BIN1 expression and a shorter disease duration, as well as a later age for its onset (Karch *et al.*, 2012). A possible connection between a higher expression of this protein and tau pathology has also been suggested (Chapuis *et al.*, 2013), due to the fact that BIN1 appears to have the ability of linking the microtubule cytoskeleton to the cellular membrane (Meunier *et al.*, 2009; Tan *et al.*, 2013).

Given that BIN1 has been implicated as having an involvement in endosome trafficking, due to the BAR-domain's ability to not only sense membrane curvature but also to induce it (Ren *et al.*, 2006), and in clathrin-mediated endocytosis (Pant *et al.*, 2009), it is an appealing thought that this protein could be involved in one of the trafficking processes that lead to the production or clearance of Aβ.

The first time that the *BIN1* gene was identified as possibly impacting the risk of an individual developing AD was through GWAS in the Genetic and Environment Risk in AD Consortium 1 study (Harold *et al.*, 2009). This protein is in fact named as the second-most prevalent genetic risk factor for LOAD, with only APOE preceding it (Calafate *et al.*, 2016). Several *BIN1* SNPs have been associated to a higher risk of AD development, however the difficulty of these studies lies in the replication of the results amongst different ethnicities (Tan *et al.*, 2013).

It is more likely that LOAD results from a combination of the effect of different gene variations, as well as environmental factors, and not just from the effect of a single polymorphism (SNP), however the study of individual SNPs is very important because it will grant us a larger understanding of the processes and pathways involved in the development of this disease.

There is also some suggestion that *BIN1* could suffer epigenetic modifications, specifically in its CpG promoter island, which could affect its expression (Tan *et al.*, 2013). This would create a disturbance in normal trafficking events, therefore would propitiating AD development. In fact methylation in this specific site was observed both in breast and in prostate cancer (Kuznetsova *et al.*, 2007).

Epigenetic alterations refer to modifications that are, like the name suggests, "above genetics". These are changes in the chromatin structure which do not result from alterations to the DNA sequence itself, and that can be transmitted to daughter cells. These modifications can include changes in DNA methylation or histone modifications, which can affect the transcription of genes (Berger *et al.*, 2009). Since altered levels of *BIN1* expression ,which could not be explained simply through sequence variation in the *BIN1 locus,* have been observed in normal aging as well as in AD brains, (Allen *et al.*, 2012), epigenetic alterations could offer an explanation for this occurrence. It is also important to note that some SNPs, especially non-coding ones, could be responsible for altering DNA methylation patterns or histone marks (Zaina *et al.*, 2010).

8. Stepping stones for this thesis

Recently, with the objective of better understanding the impact of BIN1 in Aβ production, a knockdown approach was used, resulting in novel mechanistic findings as to this protein's function. This study not only saw that BIN1 depletion led to an increase in Aβ42 specifically in axons, but also that this increase was due to an impairment in BACE1's recycling to the cell membrane (Ubelmann *et al.*, 2017).

In order for recycling to occur, tubular structures are formed, which afterwards will be cleaved and separated from endosomes. These structures are continuously formed, with one endosome being

able to originate several distinct tubules, that are then responsible for transporting the cargo back to the membrane (Weering and Cullen, 2014). Upon *BIN1* knockdown, the number and length of BACE1 tubules was seen to increase, however these carriers stayed stably attached to early endosomes instead of leading to the release of this protease (Ubelmann *et al.*, 2017). Since BACE1 is staying in early endosomes for a longer period than what happens in the normal physiological state, it remains colocalized with APP thus leading to an increase in processing and to more Aβ generation (**Figure I.3**).

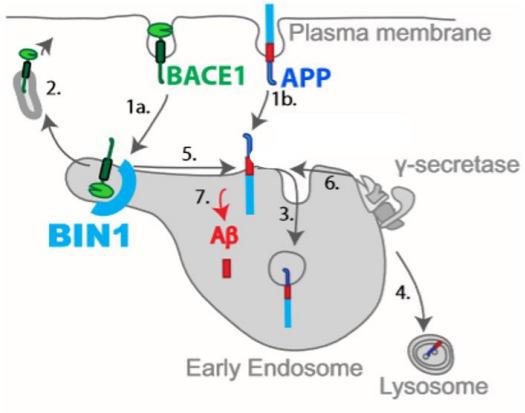

Figure I.3- Model for the role of BIN1 in Aβ endocytic generation in early endosomes. Normal APP and BACE1 endocytic trafficking diverge at early endosomes restricting Aβ generation. (1a) BACE1 endocytosis. (1b) APP endocytosis. (2) BACE1 recycling to the plasma membrane. (3) APP sorting to intraluminal vesicles. (4) APP delivery to the lysosome for degradation. (5) BACE1 cleavage of APP. (6) γ-secretase cleavage of APP-CTF. (7) Aβ generation. BIN1 is involved in BACE1 recycling to the plasma membrane, with its knockdown decreasing recycling and increasing Aβ production due to a longer co-localization time between APP and BACE1. Image adapted from Ubelmann *et al.*, 2017.

9. Objective of this study

Although BIN1 is the second-most prevalent risk factor for the development of AD, the mechanisms whereby this occurs are not well established. Recently, BIN1 knockdown (Ubelmann *et al.*, 2017) as well as its overexpression (Burrinha, 2014), were seen to lead to Aβ42 accumulation. BIN1's involvement in BACE1's recycling from early endosomes to the cellular membrane (Ubelmann *et al.*, 2017) could be the mechanism involved in controlling the amount of Aβ42 produced, eventually leading to the development of AD.

P318L and K358R are two rare *BIN1* coding mutations which have been found to be increased in frequency amongst AD patients (Tan *et al.*, 2014; Vardarajan *et al.*, 2015). P318L refers to the missense mutation in exon 11 found in Han Chinese individuals, which results in a proline to a leucine change. The change of this one deoxynucleoside (T/C) was predicted to alter BIN1's structure, affecting its function in a harmful manner (Tan *et al.*, 2014). K358R is another nonsynonymous mutation which was found to be in high frequency in LOAD cases in the Caribbean Hispanic population. This *BIN1*

mutation leads to a change from the amino-acid lysine to arginine and is predicted to be possibly deleterious (Vardarajan *et al.*, 2015).

With the objective of better understanding the impact that variants discovered in AD patients have, and through which processes they can lead to this disease, we decided to investigate the effects of these two coding mutations, P318L and K358R. We looked at BIN1 expression, Aβ accumulation, APP processing and searched for effects on early endosomes, to try and determine by which mechanisms these mutations are able to affect BIN1's normal functioning.

As such, the goal of this thesis is to assess the ability of SNPs in altering normal cell functioning and in ultimately leading to changes that could cumulate in the pathologies observed in patients with AD. In order to do so, we used both overexpression and knockdown followed by rescuing techniques in the Neuro2A (N2a) cell line which is derived from mouse neuroblastoma cells. This is a highly relevant neuronal like model and the most practical cellular system to study AD and its fundamental molecular mechanisms (Provost, 2010).

Throughout this research we will try to unveil the effects of the BIN1 mutants P318L and K358R by trying to answer some questions regarding the effect of their expression in N2a cells:

1. Do these mutations alter Aβ homeostasis?
2. If so, is there an effect in APP processing?
3. Does the expression of the mutant proteins affect actin distribution?
4. Are there any observable alterations in early endosomes?

In addition to determining whether variants of BIN1 can alone lead to AD, the ultimate goal and purpose of this work is to better understand the trafficking mechanisms through which this protein contributes to the development of this neurodegenerative disease.

II. Materials and methods

1. Cell Culture

The Neuro2A (N2a) cell line is derived from the mouse neural-crest and has been vastly used in Alzheimer's disease studies due to characteristics like its ability to differentiate into neurons and to proliferate limitlessly *in vitro* (Tremblay et al., 2010). These mouse neuroblastoma cells were cultured in a T25 flask with Dulbecco's Modified Eagle Medium (DMEM) (DMEM+GlutaMAX supplement, Gibco™, Life Tecnhologies) supplemented with 10% fetal bovine serum (FBS) (Sigma-Aldrich™) and maintained in a humidified incubator at 37°C with 5% CO_2. Once the cells reached 90% confluency the medium was removed, and the flask was washed once with phosphate buffered saline (PBS pH 7.4) (Gibco TM, Life technologies). This washing step is crucial so that dissociation of these adherent cells with trypsin (Life technologies) is made possible, since FBS inactivates this enzyme. To improve cell detachment, cells were incubated 5 minutes at 37°C with 5% CO_2. Trypsin activity was inhibited by addition of 4 mL of complete medium. Suspended cells had a round shape and were then split 1:5 to another flask to maintain culture.

Cell counting

After trypsinization and dilution in complete medium, cells were counted in a Neubauer Chamber using the trypan blue (Amresco) exclusion test to assess cell viability. Trypan blue is an impermeable dye and thus can only be taken up by cells with a compromised membrane (non-viable cells). The average of cells per square was determined and multiplied by the dilution factor and by the conversion factor for Neubauer, 10^4.

2. DNA amplification

DNA amplification was performed by transforming E.coli DH5α (Life technologies™) with the intended plasmids. Firstly, a batch of 50 µL of these competent bacteria was thawed, to which 0,5 µg of DNA was added. After 30 min of incubation on ice, the bacteria were subject to a heat shock (42°C for 45 seconds) so as to denature some of the lipids in its membrane, thus inducing the formation of pores through which DNA can enter. In order to close the pores and therefore not compromise cell viability, the bacteria were put on ice for a further 2 min.

Next, 900µL of Luria Bertani (LB medium) (Sigma-Aldrich™) was added to the bacteria and they were left to grow in a centrifuge at 200 rpm for 1 hour at 37°C. This was followed by another centrifugation, this time at 5000 rpm for 1 min, to remove most of the supernatant and obtain a concentrated batch of transformed bacteria. Re-suspended cells were then plated onto LB agar plates

with 100 µg/ mL of the antibiotic to which the construct used for transformation presented a resistance cassette. The plate was incubated overnight at 37°C.

3. Plasmid DNA preparation

To prepare the necessary plasmids to perform the experiments, a single colony of bacteria transformed with the desired plasmid and grown in a LB-agar plate, or derived from a glycerol stock, was picked with a sterile pipette tip. Said tip was then deposited in 50 mL of LB medium containing either ampicillin (100 µg/ mL) or kanamycin (100 µg/ mL), according to the plasmid's specific resistance marker. So as to promote optimum bacteria growth, the flasks were incubated at 37°C in an orbital shaker (189 rpm) for 12-16 hours.

Plasmid DNA purification from the *E.coli* DH5α cells was achieved using the NZYTech™ NZYMidiprep kit, following the protocol described in the NZYTech handbook.

Precipitated DNA was eluted in Buffer EB (Qiagen) and the DNA concentration was determined by absorbance at 260 nm, using NanoDrop 2000 UV-Vis spectrophotometer (Thermo Scientific™). DNA quality was also assessed by looking at the ratio between absorbance at 260 nm and 230 nm and between 260 nm and 280 nm.

Glycerol stocks

So as to maintain a long-term stock of the plasmid DNA, E.coli cells in exponential phase of growth (after transformation and grown in LB medium overnight at 37°C) were added to 50% glycerol in a cryovial (Thermo ScientificTM) and stored at -80°C.

4. Transient plasmid transfection

For simple immunofluorescence experiments, 70 000 N2a cells were plated per well in glass coverslips inside a 24-well plate and cultured in 500 µL of complete media in 5% CO_2 at 37 °C. After 24h of culture, cells were transiently transfected with cDNA (**Table II.1**). The amounts and volumes are given on a per well basis. For each plasmid transfection, two separate mixes were prepared, one with 0,5 µg DNA in 12,5 µL of Opti-MEM medium and the other with 0,5 µL Lipofectamine™ 2000 in 12,5 µL of Opti-MEM medium. Mixes were incubated for 5 min at room temperature, combined gently, and incubated for another 20 min at room temperature. Only 250 µL of media was left in each well and the mixture containing Opti-MEM, Lipofectamine™ 2000 and DNA was then added. Posteriorly, cells were once again incubated for 24 h at 37 °C and 5% CO_2.

For immunoblotting experiments 200 000 N2a cells were plated per well in a 6-well plate and cultured with 1,5 mL of complete media. The protocol was similar to the previously mentioned with the

only difference being the quantities of each reagent in the two mixes. In this case one mix had 2,5 µg DNA in 25 µL of Opti-MEM medium and the other has 2,5 µL Lipofectamine™ 2000 in 25 µL of Opti-MEM medium.

siRNA transfection

For immunofluorescence experiments with *BIN1* knockdown 30 000 cells were seeded for siControl coverslips and 40 000 for siBIN1 coverslips. After 24 hours of proliferation, N2a cells were transfected with 10nM of siRNA specific for *BIN1* (10µM) (GGA UCU UCG GAC CCU AUC UGT T) and non-targeting control siRNA (10µM) (UUC UCC GAA CGU GUC ACG UTT ACG UGA CAC GUU CGG AGA ATT) (Life Technologies) (**Table II.2**). The amounts and volumes are given on a per well basis. For each siRNA transfection, two separate mixes were prepared, one with 5 pmole of siRNA in 25 µL of Opti-MEM medium and the other with 0,8 µL of Lipofectamine™ RNAiMax transfection reagent (Invitrogen™, Life technologies) also in 25 uL Opti-MEM. Mixes were incubated for 5 min at room temperature before being combined and incubated for an additional 20 min at room temperature. The mixture containing Opti-MEM, Lipofectamine™ 2000 and siRNA was then added to each well and the cells were incubated at 37 °C and 5% CO_2 for 72 h. Rescue experiments were performed with plasmids containing 3 silent mutations that made them siRNA resistant, following the same protocol as previously mentioned, after 48h of incubation with siRNA.

For immunoblotting experiments 120 000 N2a cells were plated for siControl wells and 135 000 for siBIN1 wells. For each siRNA transfection, two separate mixes were once again prepared, one with 15 pmole of siRNA in 75 µL of Opti-MEM medium and the other with 2,4 µL of Lipofectamine™ RNAiMax transfection reagent (Invitrogen™, Life technologies) also in 75 uL Opti-MEM.

Table II.1- Plasmids.

Plasmid	**Obtained from**
BACE1-GFP	Gift from S.Miserey-Lenkei (Institut Curie)
Myc	Addgene
Neuronal myc-BIN1	Construct from C.Leprince (University of Toulouse)
Neuronal myc-BIN1 resistant to siBIN1	Generated by site-directed mutagenesis of neuronal BIN1-myc with five silent mutations introduced in the siRNA target sequence (primers: 5' CCGGCTGCAGAAGGACCTCCGGACGTACCTTGCTTCTGTTAA AG 3' and 5' CGCTTTAACAGAAGCAAGGTACGTCCGGAGGTC CTTCTG CAGCCGG 3')
Myc-BIN1 mutant P318L resistant to siBIN1	Generated by site-directed mutagenesis of neuronal BIN1-myc resistant to siBIN1
Myc-BIN1 mutant K358R resistant to siBIN1	Generated by site-directed mutagenesis of neuronal BIN1-myc resistant to siBIN1

Site-directed mutagenesis of neuronal *myc-BIN1* resistant to siBIN1 and the P318L mutant had already been performed and these plasmids were being maintained in the lab stock.

Myc-BIN1 K358R mutant was obtained using the NZYMutagenesis kit by nzytech™ and this process was performed with the help of Catarina Perdigão.

Table II.2- Oligonucleotides.

Oligonucleotides	**Obtained from**
siControl	GeneCust
siBIN1	Life Technologies

5. Fluorescence microscopy

Standard Immunofluorescence

After 24 hours of transfection with the chosen plasmids, N2a cells were washed in Phosphate-Buffered Saline (PBS 1X) and fixed in 4% (v/v) paraformaldehyde (Sigma-Aldrich™) in PBS for 20 minutes at room temperature. Afterwards cells were washed 3 times in PBS 1X and permeabilized in 0.1% saponin (Sigma-Aldrich™) in PBS 1X for 1 hour at room temperature. Cells were then blocked in 3% FBS in PBS 1X for 1 hour at room temperature.

Incubation time with the primary antibodies (**Table II.3**) diluted in blocking buffer depended on the objective of each experiment. Staining for Aβ42 was performed with overnight incubation at 4°C, otherwise coverslips were incubated with the primary antibody solution for 1 hour at room temperature. Washes were performed between each incubation following the same protocol as previously mentioned.

Incubation with the appropriate secondary antibodies (**Table II.4**) diluted in blocking solution were done for 1 hour at room temperature. After washing, coverslips were mounted on slides with Fluoromount-G (SouthernBiotech).

Images were acquired on a Zeiss Z2 (Carl Zeiss) upright microscope, equipped with a 60× NA-1.4 oil immersion objective and an AxioCam MRm CCD camera (Carl Zeiss), using the 63x 1.4NA Oil immersion objetive, FITC (519 nm) + CY5 (665 nm) + TRITC (576 nm) fluorescence filtersets and DIC optics, controlled with the MetaMorph V7.5.1/software. In order for the comparisons between conditions in each experiment to be valid, all samples from each experiment were imaged on the same day and with the same acquisition settings.

Table II.3- Primary antibodies.

Primary antibodies					
	Raised	Recognizes	IF dilution	WB dilution	Supplier
α-tubulin	Mouse	Mouse	All	1:10000	Millipore
Aβ42	Rabbit	Mouse, human	1:150		Genetex
APPY188	Rabbit	Mouse, human		1:1000	Genetex
BIN1	Mouse	Mouse, human		1:1000	Millipore
EEA1	Goat	Mouse, human	1:50		Santa Cruz
Myc	Mouse	All	1:500	1:500	Curie

Table II.4- Secondary antibodies and probes.

Secondary antibodies				
	Raised in	IF dilution	WB dilution	Supplier
Alexa-647 anti-Rabbit	Chicken	1:250		Molecular probes/Invitrogen
Alexa-555 anti-Goat	Donkey	1:250		Molecular probes/Invitrogen
Alexa-555 anti-Mouse	Goat	1:250		Molecular probes/Invitrogen
DAPI		1:100		Molecular probes/Invitrogen
Phalloidin-488		1:200		Molecular probes/Invitrogen
HRP anti-Mouse			1:5000	Bio-Rad
HRP anti-Rabbit			1:5000	Bio-Rad

6. Single cell quantitative analysis

Images were analyzed with Icy software (Institut Pasteur) and figures prepared in Fiji (ImageJ). To assess average fluorescence, cells were outlined using the "polygon" tool in "region of interest" and a portion of the background was also selected using the "rectangle". After exporting to excel, the average fluorescence of the background was subtracted to the average cellular fluorescence. The results were presented as percentage of the average fluorescence of cells transfected with only a Myc containing plasmid or of cells transfected with siRNA Control (100%, control).

Endosome analysis was performed using the "Spot Detector" feature under the "Detection & Tracking" tab, and the same scale and sensitivity was used throughout all images and conditions. These values were decided based on what scale and pixel number detected the largest number of obvious endosomes in all conditions.

In experiments contemplating the perinuclear area the size of the "ellipse" used for this portion of the cell was maintained in all experiments and conditions.

All graphs and statistical analysis was done using GraphPad Prism version 6 (Windows, GraphPad Software, La Jolla California USA, www.graphpad.com). Outliers were eliminated using the ROUT method. All statistical analysis for conditions that did not pass the normality tests were performed using the Kruskal-Wallis test.

7. Immunobloting

Preparation of cell lysates

72 hours after knockdown of *BIN1* and 24h after rescue with *BIN1* wt and *BIN1* mutants P318L and K358R, N2a cells were placed on ice and washed with ice-cold PBS $Ca^{2+}Mg^{+}$. Lysis buffer composed of 95% protein extraction solution (RadioImmunoprecipitation Assay (RIPA)), 4% Protease Inhibitor Cocktail (Roche Diagnostics) 25X and 1% SDS 10%, was added to cells to enable a rapid and efficient cell lysis (100 µl). RIPA solution was composed of 50mM Tris-HCl pH 7.4 (Sigma-AldrichTM), 1% NP-40 (Sigma-AldrichTM), 0.25% Deoxycholate (Sigma-AldrichTM), 150mM NaCl (NZYTechTM) and 1mM EGTA (Sigma-AldrichTM). Afterwards, cells were scrapped to ensure the complete rupture of their membranes. Protein lysates were then placed on ice for 15 min before being centrifuged at 12 000 xg for 10 min at 4°C. Supernatants were posteriorly used on Western blot assays or stored at – 80°C.

Western Blot

Protein amount from cell lysates was quantified using the Pierce™ BCA Protein Assay Kit, Thermo Scientific™.

Protein denaturation was achieved with the addition of sample buffer (Tris 0.25M pH 6.8, 40% glycerol (Sigma-Aldrich™), 8% sodium dodecyl sulfate (SDS) (Sigma-Aldrich™), Bromophenol blue 0.015% (w/v) (GE Healthcare) and 10% β-mercaptoethanol (Sigma-Aldrich™)) followed by incubation at 95°C for 5 min. Cells were separated by Tris-Glycine SDS-PAGE (running buffer: 25 mM Tris, 192 mM glycine (NZYTech™) and 0.1% (w/v) SDS), using BioRad Mini-PROTEAN™ at 90 V until the protein went past the stacking gel at which point the voltage was increased to 120 V.

Electrophoretic transfer (transfer buffer: 150mM glycine, 20mM Tris, 0.037% SDS, 20% (v/v) ethanol 96% (VWR)) to nitrocellulose membranes (0.1mm) (GE Healthcare Life Sciences) was performed at 10 V for 1h, using Bolt™ Mini Blot Module. Percentage of acrylamide (NZYTech™) gels varied between 7,5 and 15% according to the molecular weight of the proteins being analysed.

After transfer, membranes were blocked in PBS with 0.1% (v/v) Tween 20 (PBST) (SigmaAldrich™) and 5% (w/v) non-fat dry milk for 30 min at room temperature. This step is crucial

to improve result reliability as the proteins in the milk will cover the membrane surface and bind to the places where the sample proteins have not bound, thus preventing antibodies from displaying non-specific signals derived from non-specific binding.

Primary antibodies were diluted in 1% (w/v) non-fat dry milk in PBST for 1h at room temperature or overnight at 4ºC with constant agitation. After this step, and with the objective of removing any primary antibody left unbound, the membranes were washed with PBST four times for five minutes each wash. Membranes were then incubated with secondary antibody conjugated with the reporter enzyme Horseradish peroxidase (HRP), in 1% (w/v) non-fat dry milk diluted in PBST, for 1h at room temperature and with constant agitation. Membranes were once again washed following the previous protocol.

Detection of the target proteins was achieved by incubating the membranes with a mixture of equal amounts of luminol and peroxide solution, for 1 min, in a process called enhanced chemiluminescent (Amersham™ ECLTM Prime Western Blotting Detection Reagent, GE Healthcare). Luminol is oxidized to 3-aminophtalate with HRP as the catalyst, in a reaction that emits light, which is enhanced by the peroxide solution, thus allowing for the detection of the antibody-recognized proteins. The protein bands were visualized by ChemiDoc XRS+ system with exposure times varying depending on the amount of the target protein.

Analysis of protein band intensities was performed using Fiji (ImageJ) software and all graphs and statistical analysis was performed with GraphPad Prism version 6 (Windows, GraphPad Software, La Jolla California USA, www.graphpad.com").

III. Results

1. The impact of AD variants on *BIN1* expression

With the intention of understanding the effect that SNPs have, in specific the ones that lead to the *BIN1* mutations P318L and K358R, and to pinpoint whether they are able to impact the development of LOAD, we decided to assess their influence on Aβ accumulation as well as try to understand what cellular alterations they provoke that cause them to be found in association with sporadic AD.

In AD patients, *BIN1* gene expression was found increased, but the expression of BIN1 isoforms was differentially altered, with the neuronal isoform reduced and the ubiquitous increased (Calafate *et al.*, 2016). However, since it had been observed that only the neuronal isoform rescued the increase in Aβ due to *BIN1* knockdown (Ubelmann *et al.*, 2017), we decided to mutagenize the neuronal isoform in order to use it for our experiments.

With the objective of analyzing the impact of the BIN1 mutations P318L and K358R on the gene's total expression levels, we transiently transfected mouse neuroblastoma cells with myc-tagged plasmids encoding *BIN1* wild-type (BIN1 wt); *BIN1* wt siRNA-resistant, obtained by site-directed mutagenesis of the wt gene (BIN1 wt + 3sm); *BIN1* with the P318L mutation (BIN1 P318L); *BIN1* with the K358R mutation (BIN1 K358R). An empty *myc* plasmid (myc) was additionally used as a transfection control.

To measure the amount of BIN1 protein being expressed in transfected N2a cells, we performed a western blot analysis using an antibody against BIN1. The immunoblots of the two independent experiments performed are shown in **Figure III.1.A.**

In the western-blot it is possible to observe two bands for all conditions except for the lane where the lysates of cells transfected with the empty myc plasmid were run. In this lane there was an absence of bands, indicating that all bands correspond to overexpressed BIN1 and that endogenous BIN1 was not able to be detected (**Figure III.1.A**). Both bands correspond to a detection of a similar weighted protein, with the heavier band slightly above the 75 kDa and the lower-weight one slightly below this mark. We expected the detection of a single band of approximately 80 kDa, correspondent to the neuronal isoform 1 of BIN1, as the cDNA transfected encodes only for this isoform. It is therefore highly unlikely that the second band corresponds to either another BIN1 isoform or to endogenous BIN1 since, as previously mentioned, the amount of this protein was bellow detection limit in these experimental conditions.

There are several other possible explanations for the emergence of a second band. One possibility for why this occurred would be a cleavage of the target protein due to incomplete inhibition of cellular proteases. Another factor that could be influencing the molecular weight of the protein is the

existence of an interaction between our target protein and other unknown proteins or a dimerization of BIN1, however this interaction would lead to a higher increase in total molecular weight than the one observed. A third hypothesis is that some post-translational modification of the protein could be occurring, which results in a slight shift in gel migration.

Using cells expressing BIN1 wt as control, we can observe that in both individual experiments performed, an increase of 32% was observed with the expression of BIN1 P318L mutant when compared to BIN1 wt. The results from cells expressing BIN1 K358R and BIN1 wt with the 3 silent mutations varied in between experiments precluding the identification of a trend for change in expression. This lack of experimental replication was specifically denoted with the BIN1 K358R mutant, as it had an 80% difference in expression between experiments, raising the possibility of problems during the protein transfer step in the western blot (**Figure III.1.B**). More experiments are necessary to conclude on the impact of these AD mutations on *BIN1* expression. Even so, the fact that both experiments showed the same pattern with the BIN1 P318L mutant, suggests that this specific mutation does lead to an increase in *BIN1* total expression.

The densitometric analysis of the percentage of the higher band relative to the lower band in both experiments resulted in similar results. This analysis revealed that, while for cells transfected with the BIN1 wt plasmid we can observe that most of the BIN1 protein is detected in the upper range (63,5%), for cells expressing BIN1 wt with the three silent mutations there was a 50/50 split between both molecular weights. BIN1 mutation P318L seems to have led to a similar result to cells expressing BIN1 wt with the three silent mutations, with 47,7 % of the BIN1 protein being detected above the 75 kDa mark. Regarding the second mutant, BIN1 K358R, most of the protein was detected above 75 kDa, however, the difference between both molecular weights was of only 9,0% (**Figure III.1.C)**. The difference in ratio obtained between cells overexpressing BIN1 wt and BIN1 wt with the three silent mutations is surprising since the silent mutations are not supposed to alter the protein sequence, structure, interactions or post-translational modifications.

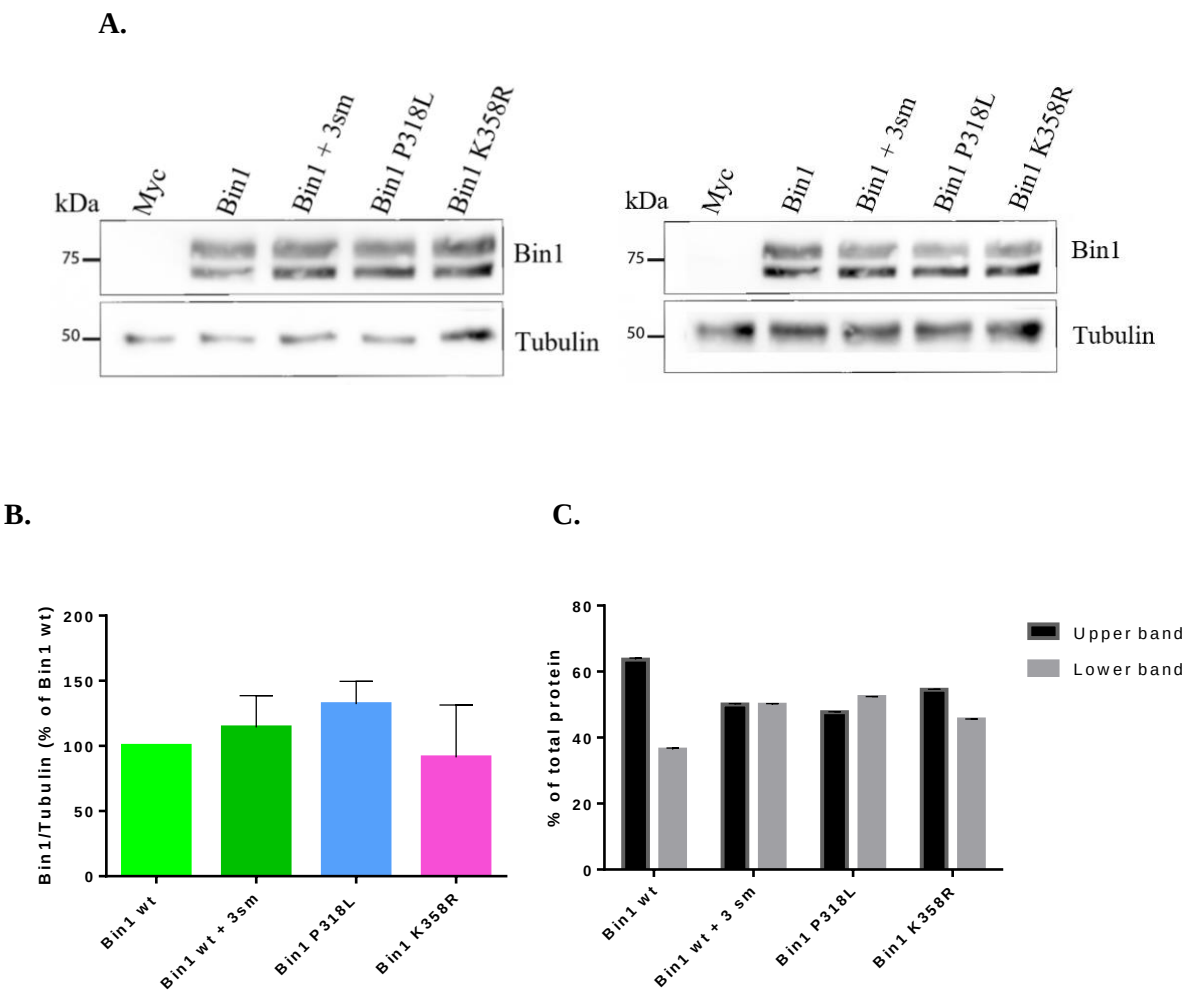

Figure III.1- *BIN1* expression levels in cells overexpressing BIN1 wt and BIN1 mutants P318L and K358R. N2a cells transiently transfected with *myc-BIN1* wt (BIN1 wt), *myc-BIN1* wt with 3 silent mutations (BIN1 wt + 3sm), *myc-BIN1 P318L* (BIN1 P318L) and *myc-BIN1 K358R* (BIN1 K358R) for 24h were analysed by western blot with anti-BIN1. Anti-α-tubulin detection was used as a loading control **A.** Western blots of lysates from two independent experiments **B.** Quantification of band densities of *BIN1* expression levels (n=2) of the western blots shown in **A**, using Fiji ImageJ software. Results were normalized by α-Tubulin and are shown as percentage of BIN1 wt (100%). BIN1 levels are increased in BIN1 wt + 3sm (114.2 ± 34.41%) and in BIN1 P318L (132.1 ± 24.86%) and decreased in BIN1 K358R (91.32 ± 56.77%). Error bars indicate SEM (Standard Error of the Mean). **C.** Ratio between the upper and the lower band observed in the western blots in **A**. Upper bands: BIN1 wt (63.64 ± 0.64%), BIN1 wt + 3sm (50.00 ± 0.41%), BIN1 P318L (47.68 ± 0.20%), BIN1 K358R (54.50 ± 0.17%); Lower bands: BIN1 wt (36.36 ± 0.64%), BIN1 wt + 3sm (50.00 ± 0.41%), BIN1 P318L (52.32 ± 0.20%), BIN1 K358R (45.50 ± 0.17%). Error bars indicate SEM.

2. Impact of *BIN1* mutant overexpression on Aβ42 levels

To determine if overexpressing P318L and K358R *BIN1* mutants leads to a similar result to the overexpression of the wt form of the protein, or whether these mutations have a greater impact in Aβ42 levels, we transiently expressed BIN1 wt, BIN1 +3sm, BIN1 P318L, BIN1 K358R, as well as a plasmid containing only myc as control, in N2a cells. After 24h of expression, we fixed the cells and stained them using antibodies against myc and Aβ42. This immunostaining allowed for observation of the

amyloid peptide distributed in puncta throughout the cells instead of in an all-over homogeneous distribution (**Figure III.2.A).** Neither overexpression of BIN1 wt nor overexpression of BIN1 mutants seem to affect Aβ42 distribution in the subcellular compartments (**Figure III.2.A**).

Quantification of the Aβ42 immunofluorescence mean intensity per single cell revealed that, as expected, there were no significant differences in Aβ42 levels between BIN1 wt and BIN1 wt with the three silent mutations (**Figure III.2.B**). However, it was still necessary to confirm these results to ensure that the silent mutations have absolutely no impact, since both mutants also carry them. Expression of the P318L and K358R mutants gave rise to a 33,6% and a 42,8% increase in Aβ42, respectively, in comparison to myc control cells. This result is significantly more than the 16,6% and 22,0% increase in Aβ42 observed upon expression of BIN1 wt and BIN1wt + 3sm, respectively (**Figure III.2.B**).

This shows that these mutations cause a larger accumulation of Aβ42 than what can be explained due to the overexpression of the BIN1 protein, with the K3558R mutant leading to almost double the increase of this peptide's levels.

A

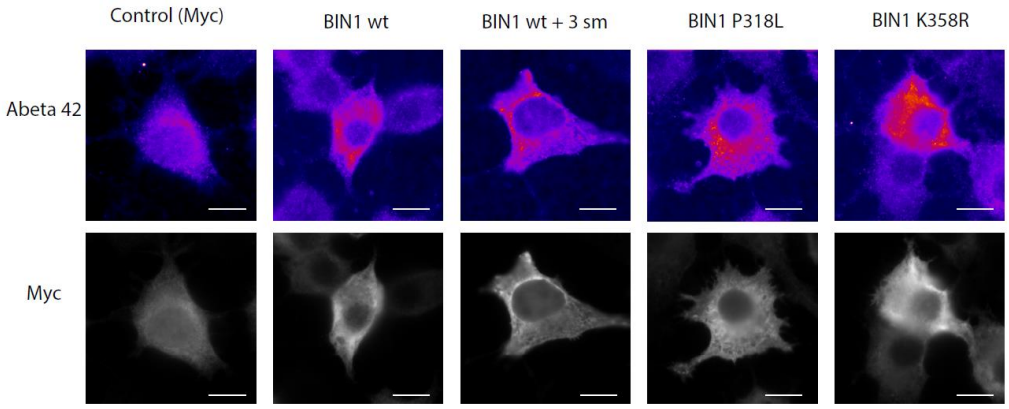

B.

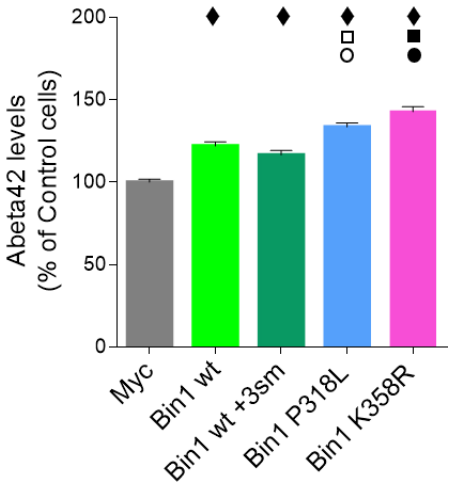

Figure III.2- Overexpression of BIN1 mutants P318L and K358R increases Aβ42 levels. N2a cells were transiently transfected with *myc-BIN1* wt (BIN1 wt), *myc-BIN1* wt with 3 silent mutations (BIN1 wt + 3sm), *myc-BIN1 P318L* (BIN1 P318L) and *myc-BIN1 K358R* (BIN1 K358R) for 24h. **A.** Representative epifluorescence images of myc and myc-BIN1-expressing N2a cells immunostained with anti-myc and anti-Aβ42. A punctate pattern of Aβ42 distribution was observed throughout the cells in all conditions. Scale bar=10µm **B.** Quantification of Aβ42 mean fluorescence in myc, BIN1 wt, BIN1 wt + 3sm, BIN1 P318 and BIN1 K358R expressing cells (210, 167, 142, 228 and 172 cells respectively; n=6) using Icy Software. GraphPad Prism 6 software was used for result analysis. Outliers were eliminated with the Rout method and the Kruskal-Wallis test was performed for statistical analysis. Results were normalized to Aβ42 mean fluorescence in myc-expressing cells (100 ± 27.03%). Aβ42 levels were increased in all myc-BIN1 overexpressing cells: BIN1 wt (122.0 ± 31.34%); BIN1 wt + 3sm (116.6 ± 31.74%); BIN1 P318L (133.6 ± 36.01%); BIN1 K358R (142.8 ±38.80%). Error bars indicate SEM. ♦ $p<0.0001$ vs myc; □ $p<0.1$ vs BIN1 wt; ■ $p<0.0001$ vs BIN1 wt; ○ $p=0.0001$ vs BIN1 wt + 3sm; ● $p<0.0001$ vs BIN1 wt + 3sm.

3. BIN1 mutants do not rescue the increase in Aβ42 levels caused by knockdown of BIN1

Previously, it was shown that BIN1 wt could rescue the increase in Aβ42 caused by *BIN1* knockdown (Unpublished data). In order to determine whether these mutations have a loss of function

effect, we decided to assess if expression of BIN1 P318L and BIN1 K358R in cells treated with siRNA against *BIN1* could also restore Aβ42 levels. This approach was also essential to be able to confirm that the results previously mentioned, relative to the increase in Aβ42, were due to the SNPs in the *BIN1* gene and not a consequence of the overexpression model.

With this immunostaining we once again observe that the Aβ42 peptide is not localized in a specific cellular compartment, following instead an all-over punctate distribution **(Figure III.3.A)**. With the myc immunostaining it is possible to see an absence of detected immunofluorescence in the first two conditions, which is expected, as cells in the siControl and the siBIN1 conditions were not transfected with any myc-tagged plasmid. Another aspect we can observe by looking at the second lane in **Figure III.3.A,** correspondent to the anti-myc detection, is that there is a difference in plasmid expression throughout the chosen representative cells, however we did not find any specific expression pattern in the different conditions.

As we can see by looking at the graph in **Figure III.3.B**, knockdown of *BIN1* caused a 24% increase in the amount of Aβ42 in cells. As already mentioned, this observation had previously been made (Ubelmann *et al.*, 2017). The re-expression of BIN1 wt had the expected rescuing effect, decreasing Aβ42 levels to a level almost identical to that of control cells. In order to have a transfection control we also transfected cells, previously treated with *BIN1* siRNA, with only the myc plasmid and, as anticipated, this did not rescue Aβ42 levels **(Figure III.3.B).**

Amazingly, not only did expression of the P318L and K358R BIN1 mutants not result in the same rescuing effect that the wt protein did, but it also caused a greater increase in Aβ42 accumulation than the one originated from the knockdown of the endogenous protein. The K358R mutant cells presented a 35% increase while the P318L ones showed an outstanding 52% increase in Aβ42 levels **(Figure III.3.B).**

A.

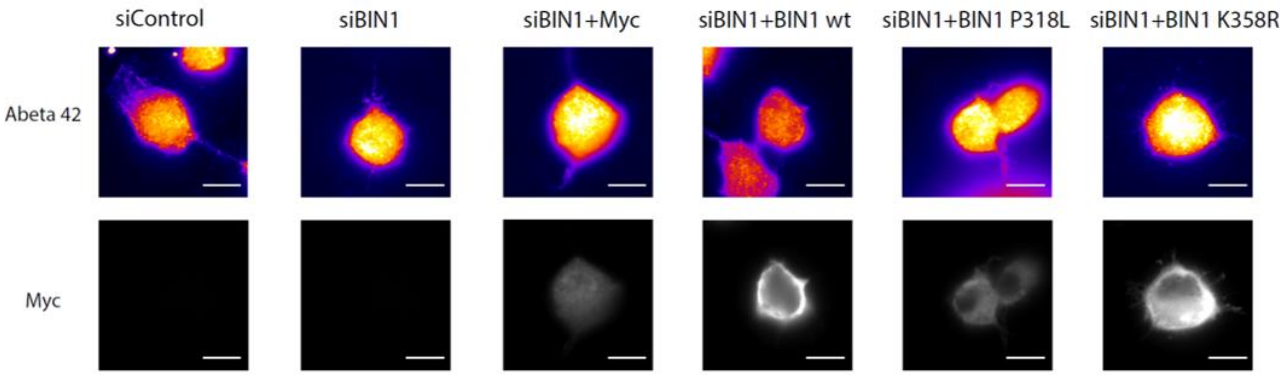

B

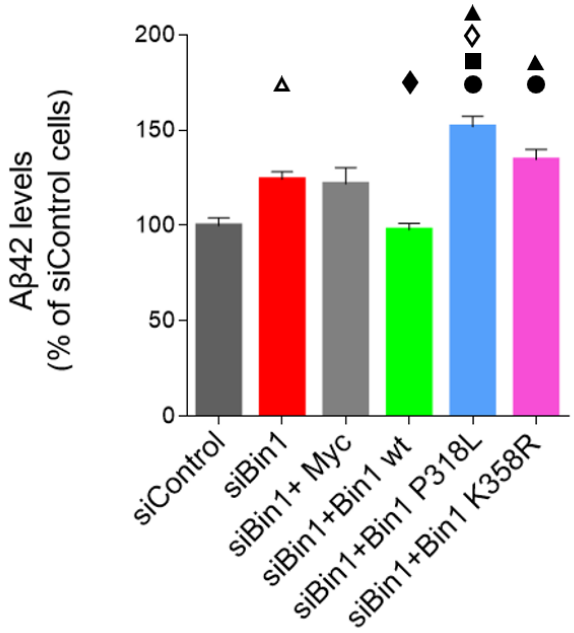

Figure III.3- BIN1 mutants do not rescue Aβ42 levels caused by *BIN1* knockdown. siBIN1 was used for 72 hours in order to silence endogenous BIN1 in N2a cells. Cells were also transfected with non-targeting siRNA control (siControl). 48h after siBIN1 treatment, cells were transiently transfected with *myc-BIN1* wt with 3 silent mutations (siBIN1+BIN1 wt), *myc-BIN1 P318L* (siBIN1+BIN1 P318L) and *myc-BIN1 K358R* (siBIN1+BIN1 K358R) for 24h. N2a cells without BIN1 knockdown (siControl) were used as a knockdown control, and cells only transiently transfected with the myc plasmid were used as a transfection control (siBIN1+ Myc). **A.** Representative epifluorescence images of N2a cells after siBIN1 treatment and plasmid transient transfection. These myc and myc-BIN1 expressing N2a cells were immunostained with anti-myc and anti-Aβ42. Scale bar=10µm **B.** Quantification of Aβ42 mean fluorescence in siControl, siBIN1, siBIN1+myc, siBIN1+BIN1 wt, siBIN1+BIN1 P318 and siBIN1+BIN1 K358R cells (75, 86, 53, 71, 69 and 55 cells respectively; n=3) using Icy Software. GraphPad Prism 6 software was used for result analysis. Outliers were eliminated with the Rout method and the Kruskal-Wallis test was performed for statistical analysis. Results were normalized to Aβ42 mean fluorescence in siControl treated cells (100 ± 34.92%). BIN1 knockdown resulted in an increase in Aβ42 levels (124.3 ± 37.06%) that was not rescued with myc expression (121.8 ± 62.37%). While BIN1 wt expression rescued Aβ42 levels (97.84 ± 27.54%), expression of BIN1 mutants P318L and K358R did not (151.8 ± 45.22%; 134.6 ± 39.65%, respectively). Error bars indicate SEM. Δ $p<0.01$ vs siControl; ▲$p<0.0001$ vs siControl; ♦ $p<0.001$ vs siBIN1; ◊ $p=0.01$ vs siBIN1; ■ $p<0.001$ vs siBIN1+myc; ● $p<0.0001$ vs siBIN1+BIN1 wt.

4. Impact of BIN1 mutants on Aβ42 perinuclear accumulation

The perinuclear region of N2a cells is where most early endosomes concentrate (unpublished observations), the preferential site of Aβ42 production (Cataldo *et al.*, 2000). Thus, we decided to investigate if BIN1 mutants are able to affect endosomal accumulation of Aβ42. For that we measured Aβ42 levels in the perinuclear region as a fraction of the total amount measured in the cell.

Observation of **Figure III.4.A** allows us to see Aβ42's distribution throughout the cell, with a higher focus near the nuclear region for cells transfected with the empty *myc* plasmid (control-a) and cells transfected with BIN1 wt (b). As for cells transfected with BIN1 P318L we can see an increase in Aβ42 all over the cell (c) with slightly more accumulation in the perinuclear area. Transfection with BIN1 K358R led to a seemingly more homogenous distribution of Aβ42, with no apparent preference for the area near the nucleus (d).

Looking at the graph in **Figure III.4.B,** we can see that the distribution of the Aβ42 signal detected in the perinuclear region in cells overexpressing the wt BIN1 protein is similar to the one found in myc-control cells, meaning that the overexpression of this protein does not alter endosomal accumulation of the Aβ42 peptide. However, when the mutant proteins were being expressed by the cells, we found a decrease in the percentage of Aβ42 in the perinuclear region. What is also very important to note is that even though they both seem to lead to a delocalization of the peptide, while the expression of the P318L mutant form of BIN1 caused a 7.5%, non-significant, decrease, the K358R mutation had double the effect, with a 15.5% decrease in Aβ42 localized in the perinuclear region of the cell. This decrease is not due to a decrease in total Aβ42 in this region in comparison to control cells, but to an increase in this peptide all throughout the cell.

These results suggest that these BIN1 mutations, specifically the K358R, have an effect in Aβ42 accumulation in the perinuclear region, which suggests an effect of these mutations in Aβ42 trafficking.

5. Impact of BIN1 mutants on perinuclear actin

Human BIN1, as well as specifically the neuronal isoform 1 which is the one we are using in this study, were seen to be able of binding to F-actin through its BAR domain (Dräger *et al.*, 2017). Since actin is required for both endosomal maturation as well as for recycling (Ohashi *et al.*, 2011), we decided to investigate whether the BIN1 mutants impacted F-actin in the perinuclear region.

Looking at **Figure III.4.A** we can see F-actin's cellular distribution (i-l), with a focus point in the perinuclear region. There does not seem to be any major actin differences in this protein's distribution throughout the different conditions.

Analysis of the mean immunofluorescence revealed a small 8% (P318L) and 7% (K358R) decrease in perinuclear actin with the expression of the mutant forms of the protein, however these

results were non-significative, and the less than 7% alteration found in the cells transfected with the BIN1 K358R mutant does not seem to correlate with the 15% decrease in Aβ42 found in the perinuclear region **(Figure III.4.C).**

A.

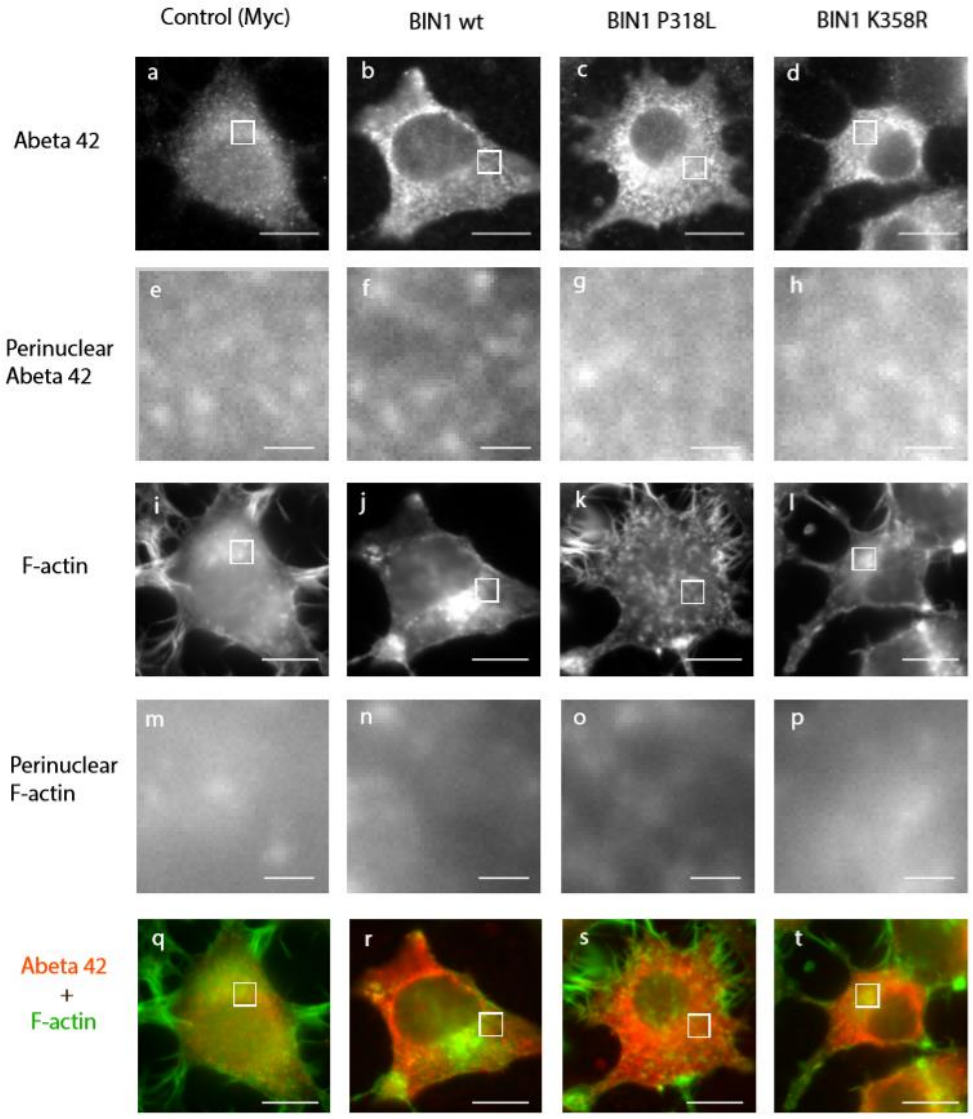

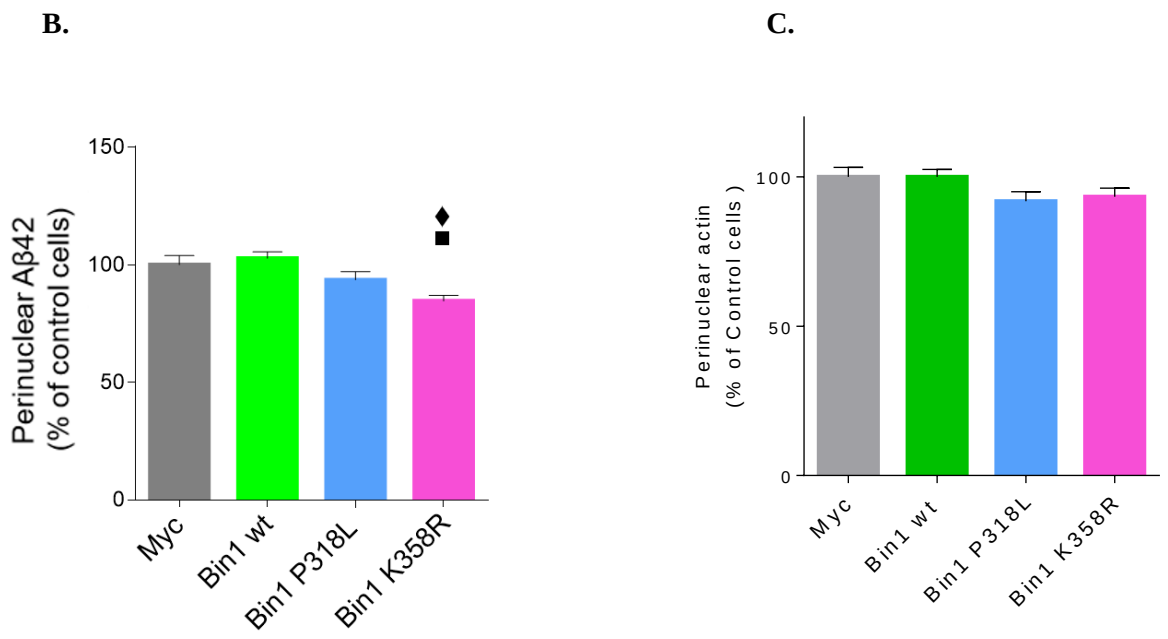

Figure III.4- Perinuclear actin and Aβ42 levels in N2a cells overexpressing BIN1 wt, BIN1 P318L and BIN1 K358R. N2a cells were transiently transfected for 24 hours with *myc-BIN1* wt with 3 silent mutations (BIN1 wt), *myc-BIN1 P318L* (BIN1 P318L) and *myc-BIN1 K358R* (BIN1 K358R). Using Icy software, a circular area near the nucleus was selected. The size of this circular area was maintained for all cells in every condition. **A.** Representative epifluorescence image of transfected N2a cells labelled with anti-Aβ42 (a-d) and anti-F-actin (i-l), with white boxes indicating magnified regions (e-h; m-p, respectively). Merged images of Aβ42 (red) and F-actin (green) are also represented (q-t). Scale bar for non-magnified regions (a-d; i-l; q-t) = 10µm; Scale bar for magnified regions (e-h; m-p) = 1µm. **B.** Quantification of the mean Aβ42 epifluorescence of the circular perinuclear area in relation to the total cellular Aβ42 levels in myc, BIN1 wt, BIN1 P318L and BIN1 K358R expressing N2a cells (67, 72, 57 and 77, respectively; n=3). Result analysis was performed with GraphPad Prism 6 and statistical analysis was done with ANOVA since these results passed the D'Agostino & Pearson normality test. Results were normalized using cells transfected with the myc plasmid as control (100.0 ± 31.59%). Aβ42 levels did not suffer any statistically relevant alterations with the overexpression of BIN1 wt (102.7 ± 23.23%) nor with the overexpression of BIN1 P318L (93.53 ± 26.53%). Overexpression of the BIN1 mutant K358R led to a decrease in perinuclear Aβ42 levels (84.57 ± 20.84%). Error bars indicate SEM. ♦ $p<0.01$ vs myc; ■ $p<0.001$ vs BIN1 K358R. **C.** Quantification of the mean actin epifluorescence of the circular perinuclear area in relation to the total cellular actin levels in myc, BIN1 wt, BIN1 P318L and BIN1 K358R expressing N2a cells (73, 70, 74 and 79, respectively; n=3). Results were normalized to myc-expressing cells (100.0 ± 27.19%). N2a cells did not exhibit any statistically relevant alterations: BIN1 wt (100.0 ± 20.64%); BIN1 P318L (91.88 ± 26.90%); BIN1 K358R (93.37 ± 25.23%). Error bars indicate SEM. Outliers were eliminated using the ROUT method.

6. BIN1 mutant's effect in endosomes

Early endosomal enlargement was observed in neurons of patients with AD, likely due to an alteration in the endocytic pathway which leads to cargo accumulation. This impairment in trafficking is a very specific and early response to AD (Cataldo *et al.*, 2000). This increase in endosome size was replicated upon BIN1 knockdown (Ubelmann *et al.*, 2017).

EEA1 is a peripheral membrane protein found co-localized with the Rab5 GTPase, meaning that it is mainly present in the membranes of early-endosomes (Mu *et al.*, 1995). With the objective of seeing if the P318L and K358R mutations recapitulated early endosomes enlargement, we immunostained transiently transfected cells for the EEA1 marker and analyzed for signal intensity, size, and number of

puncta. This immunostaining allowed for observation of the punctate distribution of the EEA1 signal, with some puncta clearly corresponding to early-endosomes **(Figure III.5.A)**. While observing **Figure III.5** we can see a decrease in signal intensity from left to right, with cells transfected with the empty *myc* plasmid (control) displaying the highest level of EEA1 intensity. It is also possible to denote a decrease in plasmid expression in the BIN1 K358R expressing-cell by looking at the anti-myc immunostaining lane, however no pattern of significant BIN1 decreased expression was detected with this or any other plasmid.

Looking at **Figure III.5.B** regarding endosome number, no significant differences were observed in comparison to control cells, which indicates that neither BIN1's overexpression nor the overexpression of the mutants interfere with early endosome number.

Regarding endosome size **Figure III.5.C**, overexpression of the wt BIN1 protein and of the K358R mutant resulted in similar endosome size to that of expression of the myc control plasmid did. In these experiments the overexpression of the BIN1 wt protein did not replicate the results obtained upon its knockdown where a significant increase in size was observed (Ubelmann *et al.*, 2017). Most surprisingly is the fact that not only did the cells transfected with the P318L mutant not show the enlargement of endosomes expected due to the increase in accumulation of Aβ42, but they in fact displayed a 15% reduction in size.

The most significant results were the ones regarding EEA1 signal intensity, as even though no significant change was seen in cells overexpressing BIN1 wt, with only a 6% decrease in comparison to control cells, in the ones expressing the mutant forms of this protein this change was a lot more obvious, with a 18% (P318L) and a 20% (K358R) decrease **(Figure III.5.D)**.

A.

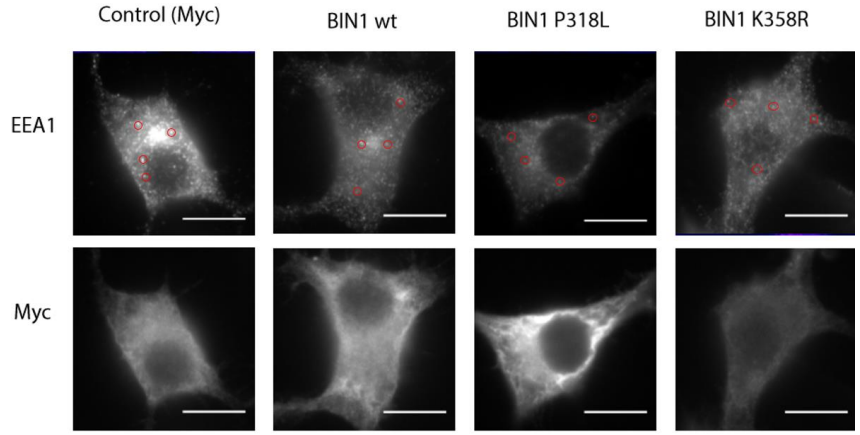

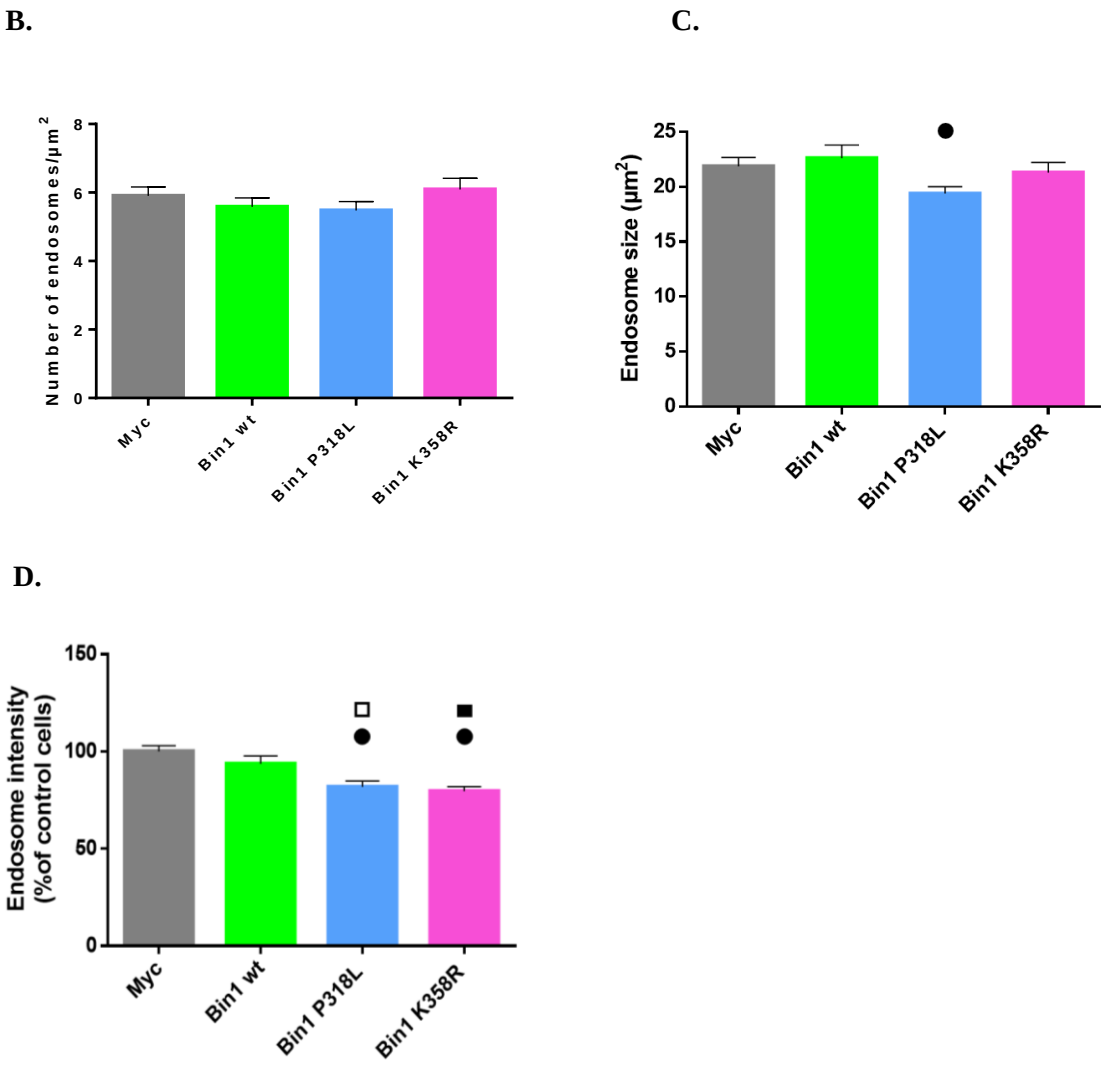

Figure III.5- Effect of BIN1 wt and BIN1 mutants in early endosome number, size and intensity. N2a cells transiently transfected with *myc* (myc), *myc-BIN1* wt with 3 silent mutations (BIN1 wt), *myc-BIN1* P318L (BIN1 P318L) and *myc-BIN1* K358R (BIN1 K358R) for 24h were analysed by immunofluorescence with anti-EEA1, an early-endosomal marker. All quantifications were performed using Icy software. Result graphing and analysis were done using GraphPad Prism 6. Outliers were eliminated using the ROUT method. Since the results passed the normality test ANOVAs were used to do multi-comparison statistical analysis **A.** Representative epifluorescence images of N2a cells after plasmid transient transfection. These myc and myc-BIN1 expressing N2a cells were immunostained with anti-myc and anti-EEA1. Scale bar=10µm. Red circles highlight examples of detected endosomes in each condition. **B.C.D.** Quantification of the EEA1 mean number of puncta, size and intensity in myc, BIN1 wt, BIN1 P318L and BIN1 K358R expressing N2a cells (68, 62, 72 and 63, respectively; n=3). Error bars represent SEM **B.** Quantification of the number of EEA1 puncta/µm^2. No statistically relevant results were obtained. **C.** Quantification of the size of EEA1 detected epifluorescence signal. Overexpression of BIN1 P318L led to a decrease in EEA1 size (19.39 ± 5.29 µm^2) in comparison to overexpression of BIN1 wt (22.61 ± 9.16 µm^2). **D.** Quantification of EEA1 signal intensity. Results were normalized for myc-expressing cells (100.0 ± 24.56%). Overexpression of BIN1 wt did not result in statistically relevant alterations in signal intensity (93.68 ± 31.40%) however, overexpression of the P318L and K358R mutants resulted in signal intensity decrease (81.87 ± 25.11% and 79.52 ± 18.64% respectively). □ $p<0.001$ vs myc; ■ $p<0.0001$ vs myc; ● $p<0.1$ vs BIN1 wt.

7. BACE1 levels in cells overexpressing *BIN1* mutants

With the knockdown of BIN1 having been shown to impact BACE1 degradation, therefore increasing its total level (Miyagawa *et al.*, 2016), and with BACE1 being the rate-limiting step for the

production of Aβ42, we decided to investigate whether the overexpression of the BIN1 mutants affect BACE1 total levels similarly to how it affects Aβ42 levels. To assess the levels of BACE1, we performed immunoblotting experiments using an antibody against BACE1 **(Figure III.6.A).**

Observing the immunoblots show in **Figure III.6.A** we can see a band at around 50 kDa in all conditions, which corresponds to the BACE1 protein. We decided to show the immunoblot result of two independent experiments, given they produced dissimilar results.

Analysis of the bands' densities showed that the amount of BACE1 in cells transfected with BIN1 wt as well as cells transfected with BIN1 wt with the three silent mutations only varied slightly from control, with a 12% increase and a 7% decrease respectively (**Figure III.6.B).** The most noteworthy results however, derived from the expression of the mutant forms of this protein, with expression of BIN1 P318L resulting in a 22% increase in the amount of BACE1, while expression of BIN1 K358R led to a 25% decrease. These results are specially interesting as even though both of these mutations have been found associated with AD and both of them lead to an increase in total intracellular Aβ42, they seem to differently affect BACE1 levels. This suggests that these mutations might contribute to the development of AD through different pathways.

A.

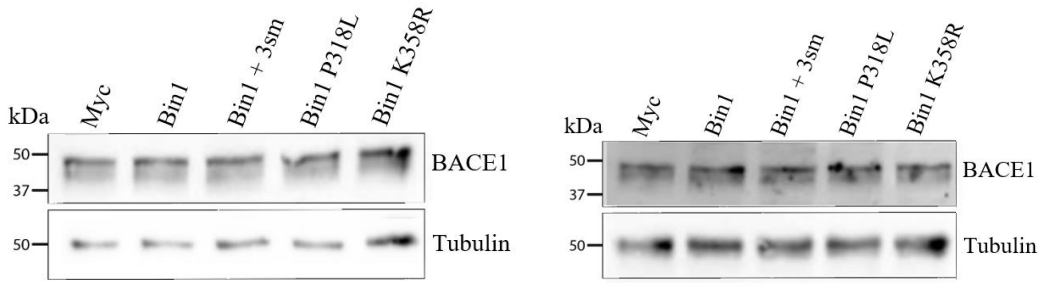

B.

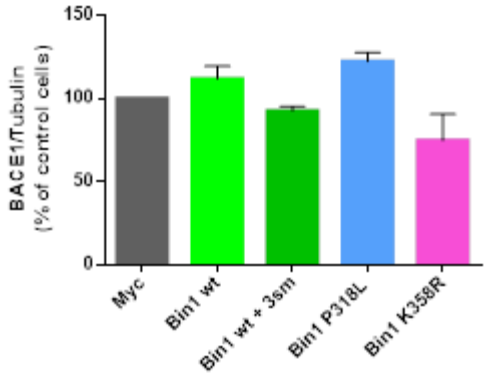

Figure III.6- BACE1 levels in cells overexpressing BIN1 wt, BIN1 P318L and BIN1 K358R. N2a cells transiently transfected with *myc* (myc), *myc-BIN1* wt (BIN1 wt), *myc-BIN1* wt with 3 silent mutations (BIN1 wt + 3sm), *myc-BIN1* P318L (BIN1 P318L) and *myc-BIN1* K358R (BIN1 K358R) for 24h were analysed by western blot with anti-BACE1, using anti-α-tubulin as a loading control. **A.** Western blots of lysates from two independent experiments**. B.** Quantification of BACE1 band densities (n=2) of the western blots shown in A, using Fiji (ImageJ) software. Results were normalized by α-Tubulin and are shown as percentage of myc (100%). BIN1 levels are increased in BIN1 wt (111.9 ± 10.70%) and in BIN1 P318L (122.3 ± 7.64%). A slight decrease in BIN1 wt + 3sm (92.63 ± 7.64%) and a more pronounced decrease in BIN1 K358R (74.92 ± 22.11%) were also observed. Error bars indicate SEM.

8. Alterations in APP processing

The first step in APP processing involves its cleaving by α or β-secretase. The carboxyl terminal fragments (CTFs) of APP, known as α-CTF and β-CTF, are further processed by γ-secretase, with the cleavage of β-CTF originating Aβ (Zhang *et al.*, 2011). It is then possible that the increase in Aβ42 observed could be explained by an increase in APP processing, which was in fact observed previously with the knockdown of BIN1 (Ubelmann *et al.*, 2017). Since the overexpression of BIN1, as well as the expression of BIN1 P318L and BIN1 K358R led to increased levels of intracellular Aβ42, we decided to investigate the impact the overexpression of these proteins have in APP processing. In order to do so we measured the levels of both APP CTFs and APP upon 24 h of overexpression of plasmids encoding BIN1 wt and mutants, as well as an empty myc vector as control, through western blot with an antibody specific for APP c-terminal domain (APP Y188) **(Figure III.7.A).** The change in APP and APP CTFs levels was quantified by densitometry of the corresponding bands relative to control (myc) as well as by calculating the ratio APP CTFs/APP which were then normalized to percentage of control (myc) (**Figure III.7.B,C**).

By looking at the western blot in **Figure III.7.A** it is possible to detect two bands, one at 100kDA and another at 15kDA. This first band corresponds to the molecular weight of full-length APP and the second lower-weight band to α and β-CTFs, of approximately 10-14kDa. It is important to note that the bands obtained in the first lane were abnormally fainter than what was usually obtained in previous experiments, indicating that a technical problem, such as incomplete transfer from the gel to the blotting membrane or a loss of sample post-quantification, resulting in a decrease in the confluency of the cells in this particular condition, might have occurred.

Looking at **Figure III.7.B,** we can see that the overexpression of BIN1 wt and of BIN1 wt with the three silent mutations led to a similar increase, of 142% and 180% respectively, in the APP CTFs/APP ratio in comparison to myc-expressing cells. This suggests that the increase in Aβ42 observed with the overexpression of the BIN1 protein is due to an increase in BACE1 processing of APP. Surprisingly, the overexpression of BIN1 P318L and BIN1 K358R proteins did not seem to increase APP processing in a significant manner, as the increase was only of 28% and 15% respectively **(Figure III.7.B**), indicating that, unlike with the overexpression of the wt protein, the increase in Aβ42 is not due to an increase in BACE1 processing.

Alterations in the APP CTFs/APP ratio could also be related to alterations in the total amount of APP available in the cells, and as such we decided to look at the levels of this protein. In **Figure III.7.C** we confirm that the levels of APP in myc-expressing cells are 4 fold less than in the other conditions. This observation was unexpected as APP is a protein which is present in high quantities in cells and thus the difference between the control and the other conditions should not be as dramatic. This supports the possibility of the occurrence of experimental errors, as previously mentioned. Given

the lack of reliability in the results from the myc-control cells we can only compare the impact of the overexpression of the BIN1 mutants with the results from BIN1 wt or BIN1 wt with three silent mutations, which both showed similar levels of APP. We observed a small 15% increase in APP levels in BIN1 P318L expressing cells and a small 12% decrease in APP levels in BIN1 K358R expressing cells, in comparison to BIN1 wt-expressing cells. More experiments are needed to determine if these variations are significant. Interestingly, although the APP total was similar in all BIN1 overexpressing cells, the levels of APP CTFs were reduced upon overexpression of the BIN1 mutant proteins when compared to BIN1 wt or BIN1 wt with three silent mutations, with a 40% decrease in cells overexpressing BIN1 P318L and a 59% decrease in cells overexpressing BIN1 K358R **(Figure III.7.C)**. These results indicate that the BIN1 mutations are altering the processing of APP but not its expression nor degradation.

A.

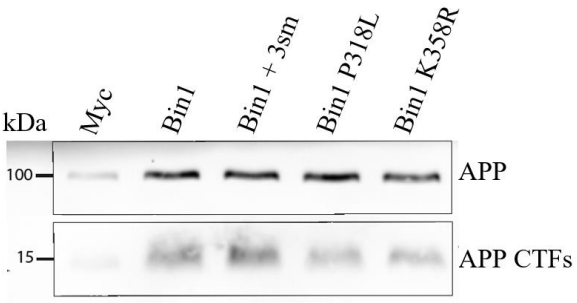

B.

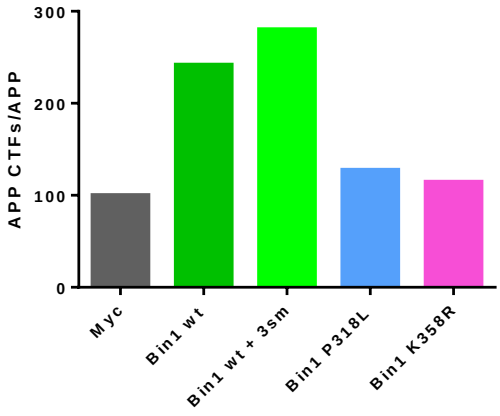

C.

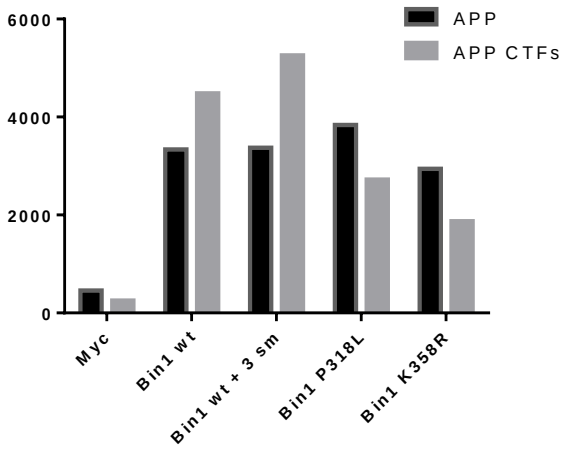

Figure III.7- BIN1 mutants do not increase APP CTFs/APP ratio. N2a cells transiently transfected with *myc* (myc), *myc-BIN1* wt (BIN1 wt), *myc-BIN1* wt with 3 silent mutations (BIN1 wt + 3sm), *myc-BIN1* P318L (BIN1 P318L) and *myc-BIN1* K358R (BIN1 K358R) for 24h were analysed by western blot with anti-APP. **A.** Western blot analysis of cell lysates from transfected N2a cells (n=1). **B.** Ratio of APP CTFs over APP band densities, normalized to the levels measured in myc-expressing cells. APP CTFs/APP ratio increased in cells overexpressing BIN1 wt (241.8%) and BIN1 wt + 3sm (280.4%). Overexpression of the mutant forms of BIN1 did not have an effect in APP processing, with results from cells overexpressing BIN1 P318L (127.6%) and cells overexpressing BIN1K358R (114.5%) remaining similar to control. **C**. Quantification of band densities of APP and APP CTFs of the western blot shown in **A** normalized to the levels measured in myc-expressing cells.

IV. Discussion

In this thesis we proposed to contribute to uncover the impact that SNPs in the BIN1 protein can have in mechanisms relevant for the development of AD, specifically of two rare coding mutations known as P318L and K358R.

Firstly, we identified a possible effect of the mutation P318L in the expression levels of the *BIN1*, leading to an increase in total protein. This is a very important factor to note, as the excess cargo might result in trafficking defects, thus affecting the whole APP processing pathway. Whether this total protein increase was due to an increase in BIN1's production or to a decrease in its clearance is unclear and further testing needs to be done in order to answer this question. The second mutant's effect on BIN1 expression still needs to be further studied, as the difference in results obtained from one experiment to the other suggests a possible experimental problem, probably during the protein transference step in the western blot, indicating a need for technique optimization. The most surprising result was the fact that two bands were detected instead of the single BIN1 band correspondent to the longest isoform, isoform 1, as this was the only one the cells were transfected with (**Figure III.1.A)**.

An explanation for the emergence of two bands is the possibility that an alteration of the protein stability is occurring. If the silent mutations that were created to make our plasmids resistant do siRNA caused the protein to be less stable, the increase in the BIN1 protein found in the lower molecular weight range would make sense given that the protein would be more prone for degradation. This hypothesis is possible given that in this particular experiment the BIN1 wt plasmid is the only one that does not contain these mutations, and that transfection with this plasmid resulted in the lowest amount of BIN1 being detected bellow 75 kDa. The impact of previously considered silent mutations has already been seen with the mutation 957T in the human dopamine receptor D2, which was found to not only lead to a 50% decrease in protein synthesis, but also to decrease the half-time life of the protein by half. Interestingly, the simultaneous expression of this silent mutation with another one known as 1101A, which alone did not affect translation activity nor mRNA stability, rescued the defects caused by 957T (Duan *et al.*, 2003). These discoveries only highlight the fact that not all silent mutations are non-functional and may in fact have an unexpected impact in the production and degradation of the final protein.

When we try and correlate both the expression results and the ratio between the upper and the lower immunoblot band **(Figure III.1.C),** we can observe that when most of the protein is detected above the 75kDa mark, the expression levels are lower than when we have more protein located below the 75 kDa mark. This might suggest that one or more of the three silent mutations in BIN1 + 3sm might lead to post-translations modifications of the BIN1 protein, which can be detected through a slight change in migration speed, with more protein being detected in the lower band than in cells transfected with BIN1 wt. This possible post-translational modification would also correspond to an increase in

protein synthesis or in protein stability, resulting in higher levels of detected BIN1. Comparison of the results obtained from cells transfected with BIN1 + 3sm with cells transfected with the mutant BIN1 eliminates the risk that what we are observing with the mutant plasmids' expression is due to the silent mutations. The fact that cells transfected with BIN1 K358R have an increase in BIN1 being detected in the upper band, as well as an expression decrease in comparison to cells transfected with BIN1 wt with the silent mutations, while the P318L mutation strengthens the effects in increased expression and increased amount of BIN1 detected above the 75 kDa mark, suggests that not only do both of these synonymous mutations affect either production or clearance of BIN1, but also that they affect the protein, and consequently the cells, through different processes.

One important aspect to explore is the possibility that, even though the silent mutations that were created in order to make our plasmids resistant do siRNA do not lead to an amino-acid change, the nucleotide change may be enough to alter the mRNA secondary structure. If this is the case, these mutations could alter the binding of different factors, leading to an impact in the speed of translation, influencing gene expression. Alterations in translation speed could result in not only differences in protein expression, but also in alterations to the protein's final structure, as a pause in any particular spot during the translation step could result in the protein folding in a way that would not happen without this event (Tsai *et al.*, 2008; Sander *et al.*, 2014; Bali and Bebok, 2015). However, given that we utilized a SDS-PAGE gel, it is not possible to assess whether there is an alteration in protein conformation, as all proteins were denatured in SDS.

Nevertheless, even with the possible effect one or more of the silent mutations introduced to the *BIN1* gene may have, by using the wild-type plasmid with these 3 silent mutations as a control, we can still uncover what possible effects the P318L and K358R mutations have than caused them to be found in high correlation with AD.

We decided to next look at whether these mutations could have an impact in Aβ42 and saw that indeed they do, with both mutants leading to an increase in the amount of this 42 amino-acid long peptide. We will have to perform further experiments to know whether this is due to an increase in production or a decrease in clearance. It is also very important to note that, since the differences in Aβ42 between cells transfected with both wt forms of *BIN1* are not significant, the silent mutations do not seem to have an impact in these results. As such, we can attribute the increase found in cells expressing the mutant forms of the protein solely to the mutations and not to an influence by the experimental model.

To further confirm the impact of the P318L and K358R *BIN1* mutations, we performed a knockdown of the endogenous *BIN1* prior to transfection. With this we were able to see that not only

are the BIN1 mutated forms not able to rescue the increase in Aβ42 observed due to the silencing of the endogenous protein, but that they also boost this effect.

Another aspect that is interesting is that, even though the differences in Aβ42 amount found between cells transfected with BIN1 P318L and BIN1 K358R is not significant in the overexpression nor the knockdown and rescue experiments, in the first experimental design we can observe that we have a slight increase in Aβ42 in cells expressing the BIN1 with the P318L mutation over the ones expressing the K358R mutation, however, in the second one this scenario is reversed. Even though the differences are not remarkable, it does raise questions relatively to how our overexpression model may be influencing the results. Nonetheless, overexpression experiments with our mutations in N2a cells are a first step to understanding the impact that P318L and K358R expression has in neurons and in what ways they can influence the development of LOAD. For instance, even through this most basic model, we were able to see that these mutations lead to an increase in Aβ42, which supports this experimental design's reliability.

The endosomal maturation process begins with endocytosis of cargo from the plasma membrane, and then it progresses inwards towards the nucleus (Pálfy *et al.*, 2012). This means that late endosomes are located nearer to the nucleus than early endosomes are, even though they all localize closer to the nucleus than the cell periphery. Aβ42 is thought to be mainly produced in early endosomes, the first convergence location for BACE1 and APP.

When looking at the enrichment of Aβ42 near the nucleus we saw that this peptide was not particularly enriched in the perinuclear region of the cells expressing the mutant proteins in comparison to control cells, specifically the ones transfected with the BIN1 K358R mutant. If these mutations caused BIN1 loss of function, they would, similarly to what was seen with the knockdown of BIN1 (Ubelmann *et al.*, 2017), lead to an impairment in BACE1's recycling to the cell membrane. As such, this would suggest an increase in total BACE1 in early endosomes and consequently, due to the increase in colocalization time between this protease and APP, an increase in Aβ42 production in early endosomes. Considering this, the decrease in perinuclear Aβ42 observed in the mutants, which indicates an increase in the outer regions of the cells, is suggestive of an increased production of this peptide, in not only early but also late endosomes, most likely due to a decrease in BACE1 clearance. Seeing as the decrease observed in cells transfected with the BIN1 P318L mutant was not as accentuated as the one in cells transfected with the second mutant plasmid, this supports different mechanistic processes through which they might lead to the increase in Aβ42 and consequently to the development of LOAD. The P318L mutation, which led to similar, if not higher, levels of total Aβ42 in cells in comparison to the K358R mutation, could lead to a longer interaction between APP and BACE1 due to longer impairment of the secretase's recycling, meaning that APP continues to be cleaved by BACE1 during endosome maturation, causing there to be more Aβ42 nearer to the nucleus and not just in the cell periphery. These

results might also indicate that there is a retention of endosomes in the perinuclear area, instead of them following their normal route.

With the interaction between BIN1's BAR domain and actin having already been established (Dräger *et al.*, 2017), and the fact that actin's inhibition leads to impairment of endosomal trafficking (Ohashi *et al.*, 2011), we wanted to see whether we could observe any differences in perinuclear actin, as this could be correlated with an impairment in BACE1 recycling. Even though we did see a slight decrease in perinuclear actin, it does not seem likely that this alteration is responsible for the delocalization of Aβ42 observed. The mutations we are studying are not located in the BAR domain, which makes them less likely to affect BIN1's interaction with this protein. Nonetheless we still need to consider the fact that if any of these mutations lead to an alteration in BIN1's conformation, they might influence its relationship with all other proteins. As such, it is possible that an alteration that we could not detect in the interaction between BIN1 and actin is responsible for a defect in tubule formation and consequently in BACE1 recycling, which in turn will lead to an increase in Aβ42 production.

With the objective of trying to understand what kind of alterations are happening in endosomes that are ultimately leading to an accumulation of intracellular Aβ42 in cells transfected with the BIN1 mutants P318L and K358R, we looked at the EEA1 signal in these cells. Even though we mainly suspected that there would be changes in the number or size of endosomes, the alterations observed in these aspects were not significant. The only significant change in endosome size was found in cells transfected with BIN1 P318L, which presented a slight reduction.

One of the earliest known responses to AD is an increase in endosome size and volume as well as an increase in Rab5 expression levels (Cataldo *et al.*, 2000; Ginsberg *et al.*, 2010). Activation of the Rab5 GTPase was seen to promote endocytosis as well as endosome fusion (Kim *et al.*, 2016), thus leading to an increase in endosome size. These results were able to be replicated upon BIN1 knockdown (Ubelmann *et al.*, 2017), as such it was surprising to find a decrease in endosome size in cells overexpressing the BIN1 P318L mutant. An explanation for this is that, while a decrease in BIN1 levels promotes an over-activation of Rab5, an increase in this protein may lead to the opposite result (Calafate *et al.*, 2016). This means that our overexpression experimental model might be leading to an inactivation of Rab5 and consequently to a decrease in endosome fusion, making it impossible for us to see whether these mutations affect endosome size. The fact that the *BIN1* P318L mutation seems to promote an increase in BIN1 expression levels correlates well with the decrease in endosome size observed in these cells, supporting this hypothesis.

The most significant difference obtained while looking at the EEA1 signal was a loss in intensity found in cells overexpressing the mutant BIN1 proteins. The EEA1 protein is responsible for several events in early endosomes like vesicle budding, transporting, tethering, and docking events (Voltan *et*

al., 2013). Since the number of EEA1 puncta does not seem to differ with the expression of the different plasmids and that the quantity of antibody used was the same in all conditions, the decrease in signal intensity might be due to a variance in antibody-epitope recognition. EEA1 is in fact a Rab5 effector and its association with the endosomal membrane was seen to necessitate Rab5–GTP activity (Simonsen *et al.*, 1998). How BIN1 overexpression is affecting the activation of Rab5 is unclear. However, one possible explanation for the decrease in EEA1 intensity is that the decrease in interaction between Rab5 and EEA1 alter the latter's conformation, causing the recognition between the antibody and the protein's epitope to be weaker than normal. As such, it would be important to try a knockdown approach of the endogenous BIN1 protein before the transient expression of these mutants in order to see whether these results are maintained or if they truly are being clouded by the overexpression of BIN1.

Given the increase in Aβ42 levels detected in cells overexpressing BIN1 wt, BIN1 P318L and BIN1 K358R, as well as the increase detected in cells expressing the mutant BIN1 proteins, after knockdown of endogenous BIN1, we decided to look for alterations in the processing of APP. Depletion of BIN1 has been reported to impact APP processing, by observation of an increase in the ratio between APP CTFs and APP. Silencing of this protein was able to increase APP processing due to a longer retention of BACE1 in the endosomal compartment, where it allowed for a longer co-localization period between this protein and APP (Ubelmann *et al.*, 2017). In this experiment we concluded that the overexpression of the BIN1 wt protein is likely to also lead to a rise in Aβ42 levels due to an increase in BACE1 processing of APP, since we also saw an increase in the ratio APP CTFs/APP. Cells transfected with the K358R BIN1 mutant presented with lower BACE1 levels, which suggests that an increase in BACE1 APP processing is not the main cause for the increase in Aβ42 levels observed in cells transfected with this plasmid.

Looking at the levels of both APP and APP CTFs individually we can see that the major difference between the results obtained from cells overexpressing the mutated protein and the cells overexpressing the wt form is in the amount of APP CTFs detected. If cells transfected with BIN1 P318L or K358R displayed more total APP than the ones expressing only the wt protein, it would be possible that this was the cause for an increase in Aβ42, as even if the APP CTFs/ APP ratio was not increased, we could still have more total APP being cleaved by BACE1. However, we only saw a slight APP increase in cells transfected with BIN1 P318L which does not seem enough to result in the levels of Aβ42 measured. This could still be a contributing factor for why we did not see an increase in the ratio of APP CTFs/APP, but observation of the low levels of APP CTFs makes this scenario less likely. Another hypothesis is that the lack of an increase in APP CTFs detected could be due to an acceleration in the processing steps, meaning that we would never have a lot of α or β-CTFs in the cells, as these would quickly be cleaved by γ-secretase, originating Aβ or p3. Instead of an acceleration in this last processing step, we could be dealing with an increase in γ-secretase, which would lead to the same

result. The fact that we observed a slight decrease in total APP in cells expressing the K358R BIN1 mutant supports this last hypothesis, as processing of APP would be the cause for this decrease.

An additional explanation could be that, due to unknown processes, there might be a decrease in APP's processing by α-secretase, which would also lead to a decrease in CTFs, as we are detecting both α-CTFs and β-CTFs. Thus, even though we could have more total β-CTFs, which are the ones processed into Aβ, we'd have less total APP CTFs. Similarly, there could be some alteration in CTFs' processing by γ-secretase, leading to a higher percentage of CTFs being cleaved into Aβ and less into the p3 fragment. However, further testing is required to see whether BIN1 is interacting with any of the other secretases instead of only affecting BACE1's recycling to the plasma membrane, as is currently thought. Furthermore, it is important to note that these results need to be corroborated through a higher number of individual experiments.

Given that we observed an increase in APP CTFs to APP ratio in cells transfected not only with the BIN1 wt, but also in cells transfected with the wt protein with the 3 silent mutations, it is noteworthy to mention that these silent mutations are not influencing these results. This means that the P318L and K358R mutations seem to be having an effect in cells which requires further testing in order to be understood.

V. Conclusion and Future perspectives

The next steps in this research would be to repeat all experiments in primary neurons and with a knockdown of the endogenous BIN1 protein, in order to achieve better result reliability. It would also be important to perform live imaging in this model to compare the localization of the BIN1 mutated proteins with the wt form, as with our model it was not possible to pinpoint BIN1 to a specific intracellular localization, with it instead being present all-over the cell.

Furthermore, we should investigate whether the mutated BIN1 proteins lead to an accumulation of BACE1 in any of the endocytic compartment and if they lead to a disequilibrium between the amount of this BACE1 that is indeed recycled back to the plasma membrane and the amount that is sent for degradation. To achieve these results, we will follow the mentioned protocol for knockdown of endogenous BIN1 followed by transient transfection with the *myc-BIN1 wt, myc-BIN1 P318L* and *myc-BIN1 K358R* plasmids, as well as transfecting with a *FLAG-BACE1-GFP* plasmid. After 24 hours of transfection, an antibody against FLAG will be added and cells will be incubated on ice for 30 min. Subsequently to removal of unbound antibodies, cells will be fixed with 4% paraformaldehyde at different time points (0',15',60', 90') so that we can follow BACE1's trafficking. We will then use primary antibodies for organelle-specific markers, in order to co-localize with BACE1, such as EEA1, Rab11, Giantin and LAMP1, to respectively label early endosomes, recycling endosomes, the Golgi apparatus, and lysosomes/late endosomes. The internalized antibody-bound complexes will then be detected by addition of fluorophore-conjugated secondary antibodies and co-localization analysis will be able to answer the initially written questions.

Another important factor to look at is whether there are any alterations regarding the number and/or length of BACE1 tubules, as an increase in both of these factors was observed after BIN1 knockdown (Ubelmann *et al.*, 2017). If indeed the expression of the BIN1 P318L and K358R mutants replicated the results obtained with BIN1 knockdown, this would suggest that the reason they cause an increase in total Aβ42 levels is due not to a change in BACE1 quantity, but due to a lack of tubule-cleavage, resulting in less recycling of BACE1 and more co-localization time with APP.

One more interesting aspect to investigate, given that we only looked at the total levels of intracellular Aβ42, would be to also look at the levels of Aβ40, as the ratio between both of these forms of the amyloid peptide has a great impact in the development of AD. It would also be pertinent to look at the levels of extracellular Aβ42 upon the mutants' expression through an Enzyme-Linked Immunosorbent Assay (ELISA) of the medium where neurons were cultured. Additionally, we could look at the levels of a longer form of Aβ, Aβ43, as this form is also hypothesized to have an impact in the development of this illness, especially since it is proposed to be even more prone to aggregation than Aβ42 (Welander *et al.*, 2009).

Lastly, we should explore whether the P318L and K358R mutations have an impact in the conformation of the BIN1 protein, as this would impact this protein's interaction with all other proteins. As a first step to achieve this, we could start by running lysates from cells transfected with BIN1wt, BIN1 P318L and BIN1 K358R in a native protein gel. Since proteins with different conformations migrate differently through the pores of the gel, this would allow us to have a rough idea of whether any major conformational changes are occurring.

With this thesis we were able to observe the impact that a single coding mutation can have in its translated protein's function. In this case, two different BIN1 SNPs found in correlation with LOAD were able to increase cellular Aβ42 levels substantially, and this dishomeostasis is certainly a big contributor to the development of this disease. The mechanisms through which the P318L and K358R mutations lead to this effect are still unclear, however they do seem to differ from one mutation to the another. Further experimentation is necessary so as to better understand the pathways involved in these alterations. Since this is a late-onset disease, the fact that we did not obtain truly dramatic results through the experiments performed is not surprising, as the time factor does play an important role in the development of this form of AD.

Even though many questions are being answered regarding the mechanistic alterations which culminate in the development of AD, a lot more light still needs to be shed regarding the late-onset form of this disease, as the predicted number of people affected by this illness continues to increase. Only by understanding the different pathways involved can we develop reliable therapeutics to try and combat this true epidemy.

VI. References

Allen, M. *et al.* (2012). Novel late-onset Alzheimer disease loci variants associate with brain gene expression.

Andersen, O. M. *et al.* (2006). Molecular dissection of the interaction between amyloid precursor protein and its neuronal trafficking receptor SorLA/LR11. Biochemistry *45*, 2618–2628.

Bali, V., and Bebok, Z. (2015). Decoding mechanisms by which silent codon changes influence protein biogenesis and function. Int. J. Biochem. Cell Biol. *64*, 58–74.

Bateman, R. J. *et al.* (2012). Clinical and Biomarker Changes in Dominantly Inherited Alzheimer's Disease. N. Engl. J. Med. *367*, 795–804.

Berger, S. L., Kouzarides, T., Shiekhattar, R., and Shilatifard, A. (2009). An operational definition of epigenetics. 781–783.

Billings, L. M., Oddo, S., Green, K. N., McGaugh, J. L., and LaFerla, F. M. (2005). Intraneuronal Aβ causes the onset of early Alzheimer's disease-related cognitive deficits in transgenic mice. Neuron *45*, 675–688.

Burrinha, T. (2014). Bridging Integrator 1 (BIN1) controls beta-amyloid accumulation in Alzheimer's disease. *1*.

Calafate, S., Flavin, W., Verstreken, P., and Moechars, D. (2016). Loss of Bin1 Promotes the Propagation of Tau Pathology. Cell Rep. *17*, 931–940.

Cataldo, A. M., Peterhoff, C. M., Troncoso, J. C., Gomez-Isla, T., Hyman, B. T., and Nixon, R. A. (2000). Endocytic pathway abnormalities precede amyloid β deposition in sporadic alzheimer's disease and down syndrome: Differential effects of APOE genotype and presenilin mutations. Am. J. Pathol. *157*, 277–286.

Chapuis, J., Hansmannel, F., Gistelinck, M., Mounier, A., Cauwenberghe, C. Van, Kolen, K. V, and Geller, F. (2013). Increased expression of BIN1 mediates Alzheimer genetic risk by modulating tau pathology. 1225–1234.

Chia, P. Z. C., Toh, W. H., Sharples, R., Gasnereau, I., Hill, A. F., and Gleeson, P. A. (2013). Intracellular itinerary of internalised β-secretase, BACE1, and its potential impact on β-amyloid peptide biogenesis. Traffic *14*, 997–1013.

Chung, C. W. *et al.* (2001). Proapoptotic effects of Tau cleavage product generated by caspase-3. Neurobiol. Dis. *8*, 162–172.

Congdon, E. E., and Sigurdsson, E. M. (2018). Tau-targeting therapies for Alzheimer disease. Nat. Rev. Neurol. *14*, 399–415.

Corder, E., Saunders, A., Strittmatter, W., Schmechel, D., Gaskell, P., Small, G., Roses, A., Haines, J., and Pericak-Vance, M. (1993). E Type 4 Allele Gene Dose of Apolipoprotein and the Risk of Alzheimer ' s Disease in Late Onset Families. Science (80-.). *261*, 921–923.

Cormont, M., Metón, I., Mari, M., Monzo, P., Keslair, F., Gaskin, C., McGraw, T. E., and Le Marchand-Brustel, Y. (2003). CD2AP/CMS regulates endosome morphology and traffic to the degradative pathway through its interaction with Rab4 and c-Cbl. Traffic *4*, 97–112.

Dräger, N. M., Nachman, E., Winterhoff, M., Brühmann, S., Shah, P., Katsinelos, T., Boulant, S., Teleman, A. A., Faix, J., and Jahn, T. R. (2017). Bin1 directly remodels actin dynamics through its BAR domain. EMBO Rep., e201744137.

Duan, J., Wainwright, M. S., Comeron, J. M., Saitou, N., Sanders, A. R., Gelernter, J., and Gejman, P. V. (2003). Synonymous mutations in the human dopamine receptor D2 (DRD2) affect mRNA stability

and synthesis of the receptor. Hum. Mol. Genet. *12*, 205–216.

Elliott, K., Ge, K., Du, W., and Prendergast, G. C. (2000). The c-Myc-interacting adaptor protein Bin1 activates a caspase-independent cell death program.

Feero, W. G., Guttmacher, A. E., and Manolio, T. A. (2010). Genomewide association studies and assessment of the risk of disease. N. Engl. J. Med. *363*, 166–176.

Ginsberg, S., Alldred, M., and Counts, S. (2010). Microarray analysis of hippocampal CA1 neurons implicates early endosomal dysfunction during Alzheimer's disease progression. Biol. … *68*, 885–893.

Gomez-Ramirez, J., and Wu, J. (2014). Network-based biomarkers in Alzheimer's disease: Review and future directions. Front. Aging Neurosci. *6*, 1–9.

Graeber, M. B., Kösel, S., Egensperger, R., Banati, R. B., Müller, U., Bise, K., Hoff, P., Möller, H. J., Fujisawa, K., and Mehraein, P. (1997). Rediscovery of the case described by Alois Alzheimer in 1911: Historical, histological and molecular genetic analysis. Neurogenetics *1*, 73–80.

Hardy, J. A., Higgins, G. A., Hardy, J. A., and Higgins, G. A. (1992). Alzheimer ' s Disease : The Amyloid Cascade Hypothesis. Science (80-.). *256*, 184–185.

Harold, D. *et al.* (2009). Genome-Wide Association Study Identifies Variants at CLU and PICALM Associated with Alzheimer's Disease, and Shows Evidence for Additional Susceptibility Genes. Nat. Genet. *41*, 1088–1093.

Hernández, F., and Avila, J. (2008). The role of glycogen synthase kinase 3 in the early stages of Alzheimers' disease. FEBS Lett. *582*, 3848–3854.

Hippius, H. (1998). Clinical research. 101–108.

Iqbal, K., and Grundke-Iqbal, I. (2008). Alzheimer neurofibrillary degeneration: Significance, etiopathogenesis, therapeutics and prevention: Alzheimer Review Series. J. Cell. Mol. Med. *12*, 38–55.

Iqbal, K., Liu, F., Gong, C.-X., and Grundke-Iqbal, I. (2010). Tau in Alzheimer Disease and Related Tauopathies. Curr. Alzheimer Res. *7*, 656–664.

Kanatsu, K., Morohashi, Y., Suzuki, M., Kuroda, H., Watanabe, T., Tomita, T., and Iwatsubo, T. (2014). Decreased CALM expression reduces Aβ42 to total Aβ ratio through clathrin-mediated endocytosis of γ-secretase. Nat. Commun. *5*.

Karch, C. M., Jeng, A. T., Nowotny, P., Cady, J., Cruchaga, C., and Goate, A. M. (2012). Expression of Novel Alzheimer's Disease Risk Genes in Control and Alzheimer's Disease Brains. PLoS One *7*.

Kim, S., Sato, Y., Mohan, P. S., Peterhoff, C., Pensalfini, A., Rigoglioso, A., Jiang, Y., and Nixon, R. A. (2016). Evidence that the rab5 effector APPL1 mediates APP-βCTF-induced dysfunction of endosomes in Down syndrome and Alzheimer's disease. Mol. Psychiatry *21*, 707–716.

Kuznetsova, E. B., Kekeeva, T. V., Larin, S. S., Zemlyakova, V. V., Khomyakova, A. V., Babenko, O. V., Nemtsova, M. V., Zaletayev, D. V., and Strelnikov, V. V. (2007). Methylation of the BIN1 gene promoter CpG island associated with breast and prostate cancer. J. Carcinog. *6*, 7–12.

Lee, S. J., Lim, H. S., Masliah, E., and Lee, H. J. (2011). Protein aggregate spreading in neurodegenerative diseases: Problems and perspectives. Neurosci. Res. *70*, 339–348.

Lewis, J. *et al.* (2001). Enhanced neurofibrillary degeneration in transgenic mice expressing mutant tau and APP. Science (80-.). *293*, 1487–1491.

Masters, C. L., Simms, G., Weinman, N. A., Multhaup, G., McDonald, B. L., and Beyreuther, K. (1985). Amyloid plaque core protein in Alzheimer disease and Down syndrome. Proc. Natl. Acad. Sci. U. S. A. *82*, 4245–4249.

Meunier, B., Quaranta, M., Daviet, L., Hatzoglou, A., and Leprince, C. (2009). The membrane-tubulating potential of amphiphysin 2 / BIN1 is dependent on the microtubule-binding cytoplasmic linker protein 170 (CLIP-170). *88*, 91–102.

Miyagawa, T. *et al.* (2016). BIN1 regulates BACE1 intracellular trafficking and amyloid-β production. Hum. Mol. Genet. *25*, 2948–2958.

Morel, E. *et al.* (2014). PI3P regulates sorting and processing of amyloid precursor protein through the endosomal system. Nat Commun *4*, 2250.

Mu, F. T., Callaghan, J. M., Steele-Mortimer, O., Stenmark, H., Parton, R. G., Campbell, P. L., McCluskey, J., Yeo, J. P., Tock, E. P. C., and Toh, B. H. (1995). EEA1, an early endosome-associated protein. J. Biol. Chem. *270*, 13503–13511.

O'Brien, R. J., and Wong, P. C. (2011). Amyloid Precursor Protein Processing and Alzheimer's Disease. Annu. Rev. Neurosci. *34*, 185–204.

Ohashi, E., Tanabe, K., Henmi, Y., Mesaki, K., Kobayashi, Y., and Takei, K. (2011). Receptor Sorting within Endosomal Trafficking Pathway is Facilitated by Dynamic Actin Filaments. PLoS One *6*.

Pálfy, M., Reményi, A., and Korcsmáros, T. (2012). Endosomal crosstalk: Meeting points for signaling pathways. Trends Cell Biol. *22*, 447–456.

Pant, S., Sharma, M., Patel, K., Caplan, S., Carr, C. M., and Barth, D. (2009). AMPH-1/Amphiphysin/Bin1 functions with RME-1/Ehd in endocytic recycling. Nat Cell Biol. *11*, 1399–1410.

Peric, A., and Annaert, W. (2015). Early etiology of Alzheimer ' s disease : tipping the balance toward autophagy or endosomal dysfunction ? 363–381.

Provost, P. (2010). Interpretation and applicability of microrna datato the context of Alzheimer's and age-related diseases. Aging (Albany. NY). *2*, 166–169.

Rajendran, L., and Annaert, W. (2012). Membrane Trafficking Pathways in Alzheimer's Disease. Traffic *13*, 759–770.

Ren, G., Vajjhala, P., Lee, J. S., Winsor, B., and Munn, A. L. (2006). The BAR domain proteins: molding membranes in fission, fusion, and phagy. Microbiol. Mol. Biol. Rev. *70*, 37–120.

Sander, I. M., Chaney, J. L., and Clark, P. L. (2014). Expanding Anfinsen ' s Principle : Contributions of Synonymous Codon Selection to Rational Protein Design Expanding Anfinsen ' s Principle : Contributions of Synonymous Codon Selection to Rational Protein Design.

Scott, C. C., Vacca, F., and Gruenberg, J. (2014). Endosome maturation, transport and functions. Semin. Cell Dev. Biol. *31*, 2–10.

Selkoe, D. J., and Hardy, J. (2016). The amyloid hypothesis of Alzheimer's disease at 25 years. EMBO Mol. Med. *8*, 595–608.

Shankar, G. M. *et al.* (2008). Amyloid-beta protein dimers isloated directly from Alzheimer brain impair synaptic plasticity and memory. Nat. Med. *14*, 837–842.

Simonsen, A., Lipp??, R., Christoforidis, S., Gaullier, J. M., Brech, A., Callaghan, J., Toh, B. H., Murphy, C., Zerial, M., and Stenmark, H. (1998). EEA1 links PI(3)K function to Rab5 regulation of endosome fusion. Nature *394*, 494–498.

Stelzma, R. A., Schnitzlein, H. N., and Murllagh, F. R. (1995). An English I ' ranslation of Alzheimer ' s 1907 Paper , " ijber eine eigenartige Erlranliung der Hirnrinde ." *1*, 429–431.

Tan, M. S., Yu, J. T., Jiang, T., Zhu, X. C., Guan, H. S., and Tan, L. (2014). Genetic variation in BIN1 gene and Alzheimer's disease risk in Han Chinese individuals. Neurobiol. Aging *35*, 1781.e1-1781.e8.

Tan, M. S., Yu, J. T., and Tan, L. (2013). Bridging integrator 1 (BIN1): Form, function, and Alzheimer's disease. Trends Mol. Med. *19*, 594–603.

Thinakaran, G., and Koo, E. H. (2008). Amyloid precursor protein trafficking, processing, and function. J. Biol. Chem. *283*, 29615–29619.

Tiraboschi, P., Hansen, L. A., Masliah, E., Alford, M., Thal, L. J., and Corey-Bloom, J. (2004). Impact of APOE genotype on neuropathologic and neurochemical markers of Alzheimer disease. Neurology *62*, 1977–1983.

Tokuda, T. *et al.* (2000). Lipidation of apolipoprotein E influences its isoform-specific interaction with Alzheimer's amyloid β peptides. Biochem. J. *348*, 359–365.

Tsai, C., Sauna, Z. E., Kimchi-sarfaty, C., Ambudkar, S. V, Gottesman, M., and Nussinov, R. (2008). Synonymous Mutations and Ribosome Stalling Can Lead to Altered Folding Pathways and Distinct Minima. Hum. Genet. *383*, 281–291.

Ubelmann, F., Burrinha, T., Salavessa, L., Gomes, R., Ferreira, C., Moreno, N., and Guimas Almeida, C. (2017). Bin1 and CD2AP polarise the endocytic generation of beta-amyloid. EMBO Rep. *18*, 102–122.

Uchihara, T. (2007). Silver diagnosis in neuropathology: Principles, practice and revised interpretation. Acta Neuropathol. *113*, 483–499.

Vardarajan, B. N. *et al.* (2015). Rare coding mutations identified by sequencing of Alzheimer disease genome-wide association studies loci. Ann. Neurol. *78*, 487–498.

Voltan, A. R., Sardi, J. D. C. O., Soares, C. P., Pelajo Machado, M., Fusco Almeida, A. M., and Mendes-Giannini, M. J. S. (2013). Early endosome antigen 1 (EEA1) decreases in macrophages infected with Paracoccidioides brasiliensis. Med. Mycol. *51*, 759–764.

Weering, J. R. T. Van, and Cullen, P. J. (2014). Seminars in Cell & Developmental Biology Membrane-associated cargo recycling by tubule-based endosomal sorting. Semin. Cell Dev. Biol. *31*, 40–47.

Weingarten, M. D., Lockwood, A. H., Hwo, S., and Kirschner, M. W. (1975). J1t). *72*, 1858–1862.

Welander, H., Frånberg, J., Graff, C., Sundström, E., Winblad, B., and Tjernberg, L. O. (2009). Abeta43 is more frequent than Abeta40 in amyloid plaque cores from Alzheimer disease brains. J. Neurochem. *110*, 697–706.

Yankner, B. A., Dawes, L. R., Fisher, S., Villa-komaroff, L., Oster-granite, M. Lou, and Neve, R. L. (1989). Neurotoxicity of a Fragment of the Amyloid Precursor Associated with Alzheimer ' s Disease (Z.

Zaina, S., Pérez-luque, E. L., and Lund, G. (2010). Genetics Talks to Epigenetics ? The Interplay Between Sequence Variants and Chromatin Structure. 359–367.

Zhang, Y., Thompson, R., Zhang, H., and Xu, H. (2011). APP processing in Alzheimer's disease. Mol. Brain *4*, 3.

Zhao, Z. *et al.* (2016). Central role for PICALM in amyloid-B blood-brain barrier transcytosis and clearance. Nat Neurosci. *18*, 978–987.